



**University of
Nottingham**

UK | CHINA | MALAYSIA

**Applicability of Low-Cost Cameras for Monitoring Suspended Sediment in Rivers
Through Close-Range Remote Sensing**

Muhammad Azamuddeen bin Mohammad Nasir

**Thesis submitted to the University of Nottingham
for the degree of Master of Research
April 2021**

Abstract

Suspended sediment in rivers is a major problem globally. Monitoring of water turbidity and suspended sediment concentration (SSC) using satellites and in-situ sampling has been used widely to assess fine sediment pollution. However, due to low image resolution, application of satellite remote sensing is limited to only large water bodies, while in-situ sampling does not provide the continuous spatial data that are needed to address certain scientific questions or management problems. This research aimed to understand the potential of using low-cost cameras to estimate SSC in smaller rivers and streams and produce reach scale 'maps' of SSC. The study consists of development and testing of statistical models to predict SSC from pixel information contained in digital images, and validation of these models through field tests. An overarching goal was to assess the transferability of models between rivers and the effects of different camera sensors on SSC predictions. Laboratory experiments developed predictive models for two cameras (Vivo V9 smartphone and DJI Mavic Pro drone). Experiments involved manipulation of SSC in a water filled tank, with images taken with each camera and over a different coloured bed at each controlled sediment concentration. Digital Number (DN) values for each bed colour, camera and colour channel combination was extracted, with Generalised Additive Models fitted to Red, Blue and Green (R, G, B) colour bands.

In general, there were significant relations between SSC and the mean DN values, with G and B most frequently providing the best fits. Relations differed appreciably depending on bed characteristics, as a function of the relative colour of the bed and the material in suspension; some relations were direct (positive) and some indirect (negative). Thus, laboratory tests indicated that predictive relations need to be developed on a river-by-river basis due to differences in bed characteristics. There were some subtle differences between the two cameras, but in general both yielded images from which SSC could be predicted reliably in laboratory conditions. However, almost all relations broke down at very high SSCs depending on the bed colour, camera and colour channel combination; once the amount of fine material in suspension exceeded a certain threshold, SSC could not be predicted reliably from DN values. The field tests demonstrated that it is possible to produce accurate maps of SSC using an orthomosaic developed directly using DN values. These involved developing a calibration relationship for SSC v DN from images collected from drone flights at 30 m height above a reach of the Semenyih River, Malaysia. This relationship successfully predicted SSC, with the B colour band providing the best fit ($R^2 > 0.86$ for the observed v predicted). The SSC map was able to shed light on the influence of a tributary on main

stem SSCs and patterns of mixing of the fine sediment delivered by the tributary. Such fine scale spatial patterns (1cm²/pixel) are evident neither from satellite data nor in-situ monitoring. The methods presented here are applicable to a variety of questions and contexts, from understanding downstream changes in SSC in glacial rivers to assessing effects of forest loss on SSC in tropical systems.

Acknowledgements

All praise to Allah Subhanahu Wa Ta'ala the Most Compassionate and Most Merciful, for giving me the blessing, strength, and endurance to complete this study. To Him we belong and to Him we shall return.

I am indebted to my principle supervisor Prof. Christopher Gibbins, who has consistently guided me not just on the aspects of this research but also taught me the skills needed to pursue in the field as an academic. I would also like to thank my co-supervisors Dr Alexander Lechner and Dr Holly Barclay for their attentive supervision and guidance. My supervisors have patiently helped me with improving my written communication skills and helped improve my self-esteem as a budding scientist to communicate the knowledge I gain to the public with confidence and clarity.

I would also like to thank my family, fiancée, and friends for continuously supporting me by providing a place to stay during the COVID19 pandemic when I was homeless and needed a roof under my head. I am also grateful to them as they have provided me a place where I can open up about my troubles and have helped me endlessly without asking anything in return. They have continuously guided me spiritually throughout my journey.

Contents

Abstract	i
Acknowledgements	iii
Contents	iv
List of Figures	vi
List of Tables.....	vi
Abbreviations and Acronyms	vii
1. Chapter 1 General Introduction.....	2
1.1. Fine sediment: Sources, significance and ecological effects	2
1.2. Monitoring SSC	4
1.2.1. Methods of monitoring SSC	4
1.2.2. Remote sensing and suspended sediment monitoring: Malaysia.....	6
1.2.3. Theoretical framework.....	8
1.2.4. Key points.....	11
1.3. Problem statement and research gaps.....	16
1.4. Research Aims and Objectives	17
1.5. Structure of the thesis	17
2. Chapter 2 Study Area and Methods.....	17
2.1. Langat Basin: rationale of study area selection.....	17
2.2. Characteristics of the Langat.....	19
2.2.1. Climate	19
2.2.2. Geology and Soils.....	20
2.2.3. Land use and Land cover	22
2.2.4. Hydrology.....	23
2.2.5. Characteristics of the study site.....	24
2.3. Methodological framework	25
3. Chapter 3 Close Range Remote Sensing of Suspended Sediment in Tropical Rivers: Determination of key drivers using laboratory experiments	27
3.1. Introduction	27
3.2. Methods.....	28
3.2.1 Experimental setup.....	28
3.2.2 Data processing and statistical analysis.....	31

3.3	Results.....	32
3.3.1	Thresholds for measurement of Suspended Sediment Concentrations (SSC) using Red, Green and Blue Digital Number (DN) values in camera images.....	32
3.3.2	Influence of camera type on estimated Suspended Sediment Concentrations using Digital Numbers from camera images	37
3.3.3	Influence of riverbed colour on estimated Suspended Sediment Concentrations using Digital Numbers from camera images.....	38
3.4	Discussion	38
3.4.1	Potential of close-range remote sensing for monitoring suspended sediments in tropical streams and rivers.....	38
3.4.2	Thresholds for monitoring of SSC using DN values	39
3.4.3	Influence of colour band on DN values.....	40
3.4.4	Influence of camera type on DN values and implications	41
3.4.5	Influence of bed colour on DN values.....	42
3.5	Conclusion.....	43
4.	Chapter 4 Application of aerial surveys to develop suspended sediment maps of river reaches.....	44
4.1	Introduction	44
4.2	Materials and Methods	45
4.2.1	Study site.....	45
4.2.2	SSC Measurements	46
4.2.3	UAV Imagery Acquisition	47
4.2.4	Calibration, Validation and Production of Orthomosaic.....	47
4.3	Results.....	48
4.3.1	Orthomosaic	48
4.3.2	DN v SSC Calibration and Validation	50
4.3.3	Spatial Distribution of SSC.....	51
4.4	Discussion	53
4.4.1	Spatial Distribution of SSC.....	53
4.4.2	Mapping SSC Distribution in small rivers	54
4.4.3	Use of fine-scale SSC maps for ecology and conservation	55
4.5	Conclusion.....	56
5.	Chapter 5. Conclusions	58
5.1	Synthesis	58

5.2	Limitations	59
5.3	Future Research.....	59
5.4	Concluding remarks.....	61
	References	62
	Appendices	72

List of Figures

Fig. 1.1.....	4
Fig. 1.2.....	13
Fig. 2.1.....	18
Fig. 2.2.....	19
Fig. 2.3.....	21
Fig. 2.4.....	23
Fig. 2.5.....	26
Fig. 3.1.....	30
Fig. 3.2.....	31
Fig. 3.3.....	34
Fig. 3.4.....	36
Fig. 4.1.....	49
Fig. 4.2.....	50
Fig. 4.3.....	51
Fig. 4.4.....	52
Fig. 4.5.....	55

List of Tables

Table 1.1.....	14
Table 2.1.....	21
Table 3.1.....	30
Table 3.2.....	35
Table 3.3.....	37

Abbreviations and Acronyms

BIC	Bayesian Information Criterion
CMOS	Complementary Metal Oxide Semiconductor
CDOM	Coloured Dissolved Organic Matter
DN	Digital Number
EDF	Estimated Degrees of Freedom
GAM	Generalised Additive Model
GCP	Ground Control Points
JPEG	Joint Photographic Experts Group
LOI	Loss of Ignition
LULCC	Land Use and Land Cover Change
RGB	Red, Green, Blue
SSC	Suspended Sediment Concentration
TSS	Total Suspended Solids
UAV	Unmanned Aerial Vehicle

1. Chapter 1 General Introduction

1.1. Fine sediment: Sources, significance and ecological effects

Sediments play an important role in shaping the geomorphic conditions of river systems, influence their ecological inhabitants and play an important role in providing natural resources for human livelihoods. Sediments provide structure for fluvial forms such as floodplains and mudflats and organic material in suspension provides nutrients for freshwater and marine ecosystems (Kondolf et al. 2014). Catchments produce sediment that is delivered to channels via a variety of processes and routes. Once in the channel, this material is transported downstream in ways governed by the interaction of flow magnitude, channel gradient, sediment size and cohesive properties. A river's sediment load can be broken into dissolved, suspended and bedload. This thesis focuses on suspended fine sediment and stems from the need to monitor its spatial and temporal dynamics.

Globally, the fluvial system contributes an estimated 13.5-22 billion tonnes of fine sediment per year to the oceans (Holeman 1968; Syvitski et al. 2005; Walling 2006), making up an estimated 90-95 % of the total sediment flux (Vörösmarty et al. 2003). This overall flux is affected by two dominant anthropogenic factors which act in opposite ways. Land use and land cover change (particularly deforestation and intensive agriculture) has led to increases in soil erosion and delivery to the river system which magnifies the effects for small to medium-sized catchments (Dearing and Jones 2003). This is countered by the presence of barriers such as dams that retain fine sediment with great efficiency and so can result in sediment starvation in downstream reaches.

Anthropogenic activities have greatly increased the sediment flux into river systems (Syvitski and Kettner 2011) with the anthropogenic annual sediment load estimated at 15 ± 0.5 Gt/year (Syvitski et al. 2005 as cited in Syvitski and Kettner 2011). The major cause of anthropogenic river sediment loads is Land Use and Land Cover Change (LULCC), notably deforestation, conversion of pastureland to cropland and mining activities. Sediment from LULCC is expected to rise as the human population increases and countries undergo economic development. There are an estimated 50 000 large dams globally of heights greater than 15 m (Berga et al. 2006) with China having over 22 000 dams which consist of nearly half of global dams (Berga et al. 2006; Hu et al. 2009). Dams can trap up to 80% of all sediment (i.e. coarse and fine material; Hu et al. 2009; Tena and Batalla 2013) and it is estimated that 30% of the global sediment flux is trapped in reservoirs (Vörösmarty et al. 2003). These apposing influences affect

river sediment budgets, with implications for the physical and ecological character in river systems.

Fine sediment plays a major role in determining the suitability of rivers and streams for aquatic organisms. Unchecked, it is considered one of the major forms of aquatic pollution due to its detrimental effects on ecosystems and impacts on people through, for example, increased water treatment costs

Fine sediments in the water column increase turbidity and limit light penetration, reducing the population of photosynthetic organisms in the upper water column and, in turn, impacting the food chain (Van Nieuwenhuysse and LaPerriere 1986; Davies-Colley et al. 1992). High concentrations of fine sediments cause physical problems for benthic organisms such as gill abrasion which may be compounded by ingestion of harmful chemicals bounded to fine sediment (e.g. heavy metals may bind due to the tendency of fine sediment to flocculate and coagulate) (Kemp et al. 2011; Zhang et al. 2014). When deposited, fine sediment greatly modifies the substrate by altering its surface conditions (Graham 1990). The deposition of fine sediments can smother riverbed surfaces which inhibits the growth of periphyton, an important food source for invertebrates (Kemp et al. 2011), as well as changing channel morphology (Nuttall 1972; Doeg and Koehn 1994) and clogging the interstices between substrate clasts (Kemp et al. 2011).



1.2. Monitoring SSC

1.2.1. Methods of monitoring SSC

Monitoring of fine sediment is necessary to assess changes in the physical and ecological health of rivers and coastal ecosystems and provide the foundation for developing river management designed to mitigate problems. Fine sediment monitoring stations have existed in many countries for decades, mainly as part of hydrometric networks established by government agencies. Paradoxically, these stations tend to be sparse in regions where they are needed most - tropical areas where the interaction of soil type and rainfall intensity can give rise to naturally high rates of sediment runoff, but also where this runoff is being increased by activities such as land clearance, logging and urbanisation or where river sediment loads are being altered by damming (Julien and Shah 2005). The result is that in areas where rapid changes in fine sediment

concentrations are occurring, agencies may struggle to formulate comprehensive mitigation plans due to insufficient data.

Monitoring stations mostly use continuously logging sensors to record turbidity, which is then used to estimate Suspended Sediment Concentration (SSC) via a calibration relationship. In other instances, SSC is quantified from water samples which are filtered and weighed. The former method provides the high temporal resolution data that are needed to compute fine sediment loads and budgets (Béjar et al. 2017; Marteau et al. 2017a), but it is limited in spatial coverage by the high cost of deploying loggers at more than a few sites. The latter method is time-consuming and constrained by its typically low spatial (small numbers of sites) and temporal (intermittent sampling) resolution.

To address these issues, methods have been developed within the past few decades to utilise various remote sensing spectral sensors to quantify fine sediments. These have mostly used Earth observation satellite data, to assess fine sediment in deltaic floodplains (Dang et al. 2018), reservoirs (Ritchie et al. 1976), large freshwater lakes and wetlands (Mertes et al. 1993) or coastal areas (Liedtke et al. 1995; Hoguane et al. 2012) for example. A key limitation of Earth observation data for monitoring SSC in rivers is that its application is restricted to larger systems, where river width is significantly wider than pixel size (i.e. > 2m or larger river width for quantifying SSC using Landsat images) (Isidro et al. 2018; Gallay et al. 2019).

Recent studies have tested aerial and close-range (i.e. on the ground) remote sensing approaches, including images taken from bridge vantage points looking down on the water surface of rivers (Mosbrucker et al. 2015) or captured using consumer-grade cameras attached to drones (Vogt and Vogt 2016). Parallel work has demonstrated that it is possible to estimate SSC from both standard and modified cameras, including smartphone cameras (Bejestan and Nouroozpour 2007; Mosbrucker et al. 2015; Haque and Adhikary 2016; Leeuw and Boss 2018). The ubiquity of digital cameras, and especially in smartphones and drones, opens the potential for extensive 'citizen science' monitoring of suspended sediments in rivers that could provide valuable data in countries where existing water monitoring networks are sparse.

In a digital image, primary colours (Red, Green and Blue (RGB)) are separated into each colour component for each pixel. The pixel value is a vector of all three numbers. Digital number (DN) is a generic term for pixel value and is commonly used to describe uncalibrated pixel value. Reflectance measures the proportion of radiation striking a surface which is reflected by the subject of interest (Schaeppman-Strub et al. 2004). Reflectance values are calculated from DN values which have been calibrated to remove the effects of variation in surface illumination due to the angle of the sun, cloud cover and atmospheric distortion. Existing methods for determining

SSC from remote sensing images rely on reflectance values rather than the more direct use of DN values. The use of DN values would avoid the need for the collection of calibration data, making the use of digital images in citizen science water monitoring projects more straightforward.

The proliferation of mobile apps suggests that they may have utility for citizen science assessments of SSC using smartphones. Leeuw and Boss (2018) developed a protocol for estimating SSC from reflectance values using a smartphone camera but this was rather cumbersome, requiring multiple images (including of the sky) and grey balance that was then used for correction that deals with the influence of ambient conditions as seen in the equation below

$$R_{rs} = \frac{L_t - \rho L_s}{R_{ref} L_c} \quad (1)$$

Where R_{rs} refers to the above water remote sensing reflectance (sr^{-1}), L_t is the radiance leaving the water surface, L_s is the sky radiance, R_{ref} is the irradiance reflectance of a reflectance standard (grey balance), L_c is the measured radiance leaving the reflectance standard, and ρ is the sea surface reflectance factor. The protocol then derives a correlation with the suspended sediment which it itself is derived from turbidity values (NTU). Simpler methods - using DN values directly to estimate SSC - would ease application, but tests of such methods are currently lacking.

Section 1.2.3 discusses in detail the theoretical framework that serves as the foundation to this study. This theory concerns (1) how materials in a water column interact with light and in particular the interaction of light with suspended sediment, and (2) the factors that influence the how light reflecting off suspended sediment may be detected by remote sensing sensors. Before this, however, it is useful to consider the Malaysian context, to help establish the importance of the current work.

1.2.2. Remote sensing and suspended sediment monitoring: Malaysia

The Environmental Quality Act 1974 has become the key policy driver in Malaysia to ensure the protection of freshwater ecosystems. This has led to the continuous effort of the government to monitor suspended sediment dynamics, supplemented by various research projects conducted by various high level institutions, to understand, manage and mitigate the impacts of anthropogenic activities on catchment systems. Various models have been applied in order to properly understand catchments processes and dynamics, including SWAT (Lai and Arniza 2011; Khalid et al. 2016), numerical models (Toriman et al. 2010; Talib et al. 2012) and erosion models (Teh 2011; Anees et al. 2018). These models require spatial and temporal data on a range of variables

(depending on their respective purposes), including precipitation, temperature, wind speed, soil, and topographic data, and some require in-situ measurements for model calibration and validation. Some work using remote sensing-based approaches has been undertaken in Malaysia, including studies centred on coastal regions with dense populations such as the Langkat estuary, Selangor (Othman et al. 2004), the coast of Penang (Lim et al. 2008; Asadpour et al. 2012), the coast of Langkawi, Kedah (Alasloo et al. 2013), and the coast of Johor (Nichol et al. 1993a; Nichol et al. 1993b). The coastal focus is consistent with the spectral resolution of the satellite sensors (>15m) and hence best suited to monitoring larger areas. Studies focusing on remote sensing of suspended sediment in inland waterbodies in Malaysia are lacking, with existing work and mainly focuses on large waterbodies such as reservoirs and lakes (Wan Mohd et al. 2007).

While models such as SWAT have been used to help assess river fine sediment loads and budgets in Malaysia, they have a different purpose and generate data at a different spatial scale to the current study. These models are designed to understand the effects of land cover and land cover change on fine sediment loads and budgets. They can help understand sediment yield from catchments and how this influences the amount of material conveyed by the channel. SWAT is designed to be a catchment-scale tool, and is not capable of predicting fine spatial scale variation (sub-metre) in SSC. As of now, there have been no studies in Malaysia that utilised digital cameras to estimate SSC in small (1st and 2nd order) streams and rivers.

This thesis will contribute to the growing literature in monitoring suspended sediment in smaller rivers and streams; this is important not least because of the abundance of small rivers (as per Horton's Law of stream numbers). Its contributions will be: 1) the application of low-cost camera sensors from smartphones and commercial drones to estimate SSC in smaller watercourses, and 2) assess the possibility of using uncalibrated pixel values (DN) as opposed to the widely used calibrated reflectance values. The following section explores the theory that influences the possibility is using DN values directly. Fig. 1.2 represents this theory diagrammatically – it shows how various factors influence the signal received by a sensor being used to assess suspended material present in river channels.

1.2.3. Theoretical framework

Material present in water (e.g. chlorophyll a, SSC) can significantly change its backscattering characteristics (Kirk, 1994). Remote sensing techniques depend on the ability to measure these changes in the spectral signature backscattered from water and relate them by analytical or empirical models to the water quality parameter of interest (Ritchie et al. 2003). The optimal wavelength used to measure a water quality parameter is dependent on the substance or material of interest, its concentration, and the sensor characteristics. The signal reflected from suspended sediment has been shown to be within the Near Infrared (NIR) spectrum under laboratory conditions (Witte et al. 1941; Qu et al. 2014). In terms of suspended sediment, there are a number of factors that can theoretically influence the signal. Table 1.1 provides summary information on the key aspects of the literature that has used remote sensing to assess fine sediment, and which can therefore influence the relationship between DN and SSC derived from images taken from a close-range - above the water surface. Fig. 1.2 illustrates these factors schematically. Factors can be grouped according to whether they relate to hydrogeomorphic conditions (e.g. river depth, sediment, and bed sediment colour) or those internal factors (related to the camera and sensor) or external factors (ambient conditions) that influence image characteristics. The following sections provide further details on each of these factors.

‘Suspended Sediment Colour’, ‘Bed Colour’ and ‘River Depth’ interact with each other to determine the apparent colour received by the camera sensor and translated as a DN value. For the purpose of this thesis, these factors are referred to collectively as ‘River Colour.’ The interaction (relative values) of these factors influences the direction of the relationship between SSC and DN. Dark-bed colour (i.e. low DN), when combined with a light-fine sediment colour (high DN), would yield a positive relationship. This is because when the relative colour values of the light-fine sediment increases, the influence of the dark-bed colour decreases. Conversely, a light-bed colour (high DN) when combined with a dark-fine sediment colour (low DN) would yield a negative relationship. The negative relation arises because as the relative colour of the dark-fine sediment increases, the influence of the light-bed colour decreases. River Depth adds another layer of complexity as the apparent “Darkness” or “Lightness” of Bed Colour is determined by the distance of the bed from the water surface. This is because as the depth increases, a greater amount of light spectrum is absorbed by the water column, reducing the amount of light reflected off the riverbed – thus, deeper water appears darker. As the depth continues to increase it will reach a certain point where light can no longer reach the riverbed, so the bed colour no longer influences the signal (Geyman and Maloof 2019).

Another group of factors that affect the signal are grouped here under the term 'River Physiography'. The factors include 'Benthic Sediment Composition', 'Bed Topography', 'River Width' and 'Suspended Sediment Composition'. These parameters reflect the physical environment of the catchment, in terms of the geological composition of sediment, how the flow regime and valley form influence channel type and in turn bed forms and topography, and the relative balance of organic and inorganic material in the suspended load. As seen in Fig. 1.2, the 'River Physiography' does not directly influence DN values but instead interacts with other factors by way of influencing the overall colour such as how both the 'Benthic Sediment Composition' and 'Bed Topography' effect the overall 'Bed Colour' under the factor 'River Colour'. 'River Physiography' also affects the quality of the DN values as seen with 'River Width' which influences the effects of 'Riverbank Shading'.

The influence of 'River Physiography' by way of colours is largely influenced by the inorganic and organic material and also the roughness and smoothness of the bed stemming from the basin's geology. 'Benthic Sediment Composition' and 'Bed Topography' are parameters that interact together to determine the "Lightness" and "Darkness" of 'Bed Colour'. 'Benthic Sediment Composition' refers to the ratio of organic and inorganic material found in the bed which determines the overall Bed Colour. A study conducted by Tolk et al. (2000), found that white riverbed sediments had minimal influence on surface reflectance in the visible spectrum when SSC was >100 mg/L, but black riverbed sediments can increase surface reflectance in the blue and green bands.

Microscale 'Bed Topography' may influence the signal because of the influences of shadows caused by individual clasts. This shading effect of the bed darkens the tone of the overall colour of the bed (Geyman and Maloof 2019) thereby making the 'Bed Colour' signal in the DN values appear darker. Furthermore, 'Bed Topography' effects the quality of DN within the factor 'Water Surface' specifically 'River Surface Morphology' by inducing the rippling effect on the river surface which causes light reflection on the water surface – preventing image capture of the water surface.

'Suspended Sediment Composition' determines the "Lightness" and "Darkness" of 'Fine Sediment Composition'. This is driven by the ratio of organic and inorganic material suspended in the water column. Organic and inorganic material interact differently with light and its ratio determines the overall colour of fine sediment. Rochelle-Newall and Fisher (2002), found that Coloured Dissolved Organic Matter (CDOM) changes the light field by absorbing shorter wavelength light (Blue spectrum). Whereas model estimation of inorganic matter is strongest with longer wavelength (Red spectrum) (Kobayashi et al. 2011).

Lastly, 'River Width' affects the quality of DN within the factor 'Image Analysis' specifically the parameter 'Riverbank Shading'. Narrow rivers maybe completely or partially shaded or obstructed (preventing image capture of the water surface) by vegetation and/or man-made structures whereas wide rivers offer a larger surface area for images to be captured that are not shaded nor obstructed.

'Image Analysis' refers to three factors: 'Water Surface', 'Environmental Conditions' and 'Camera Specification and Use'. These factors can potentially lead to inaccuracies or uncertainties in the relationship between SSC and DN by causing changes in DN which are not related to changes in SSC. 'Water Surface' has two parameters: 'River Surface Morphology' and 'Riverbank Shading'. This parameter includes any forms of disturbances on the water surface that prevents the capturing of accurate DN value of the water surface. River Surface Morphology pertains the influence of ripples and pools which affect the attenuation of light (France 1993). Ripples cause uneven surfaces that reflect light on the water surface preventing light to interact with the water column and causes sun glint (France 1993). 'Riverbank Shading' on the other hand pertains to the influence of shadows formed by vegetation or man-made structures that cast shadows onto river surfaces. These shadows block direct light from hitting the water surface (Shahtahmassebi et al. 2013) and may cause an inaccurate representation of the river sediment in its DN. As discussed previously, the effect of shading is determined by the river width as well as by riparian land cover.

'Environmental Conditions' such as: 'Sun Angle' and 'Cloud Cover' can impact the quality of DN values. 'Sun Angle' involves the influence of specular reflection of direct solar beam from the water surface into the sensor also known as sun glint (Mount 2005; Overstreet and Legleiter 2017). Sun glint thus occurs in an image when the sensor's viewing angle is equal to the angle of reflection of the direct solar beam. Image capture of the river is best conducted when the sun angle is at 45° or lower to prevent reflected light (from the direct beam) from passing under the field of view (Mount 2005; Overstreet and Legleiter 2017). For high-elevation remote sensing such as satellites, Cloud Cover physically blocks the view of the study area. This problem does not occur for low-elevation remote sensing such as drones, as the images are taken below the clouds. However, cloud cover produces blurring of the images as it scatters light and absorbs incident light (Kokhanovsky 2004; Li et al. 2019). Cloud cover also changes the ambient lighting of the study area. These changes in ambient lighting may vary throughout the day and between sampling visits as cloud cover changes; this may lead to inconsistent image quality across a temporal scale.

A final factor is 'Camera Specification and Use' which contains parameters related to the digital technology that influence the images and results of subsequent analysis. 'Spatial Resolution' is a measure of the smallest object that can be resolved by the sensor. The higher the

spatial resolution the finer the detail that can be measured. This can be improved by increasing the number of pixels in a camera sensor or by capturing the image of the subject from a shorter distance above the water surface. ‘Spectral Resolution’ refers to the ability of the sensor to define spectral intervals such as Red, Green, Blue, Near-infrared etc. The finer the spectral resolution the better the sensor at detecting unique spectral wavelengths that respond to the subject of interest (Novo et al. 1989). Han et al. (1994) found that Near-Infrared radiation can be used to measure chlorophyll in suspended sediment. Table 1.1 (‘Selected Band’ column) gives details of the spectral bands used in different studies. In general, remote sensing instruments without the capacity to detect different spectral bands may be less suitable for quantifying SSC. Due to the different conditions and circumstances in the environment, sensors that can capture a number of bands has a greater likelihood of detecting relationships in the study area. Finally, ‘Image Processing and Storage System’ is the ability of the sensor to store large amounts of information without compromising its quality. This quality pertains to the amount of information such as highlights and shadows, dynamic range, white balance etc. An image stored as a raw file loses little information while a JPEG file pre-processes the images leading to a decline information and flexibility for later processing (Yuan and Sun 2011). This means that in the raw file, there is an opportunity to recover information from underexposed or overexposed images which are not possible for JPEG file. The downside is that images in raw occupy a lot of memory space as compared to JPEG files which is why it is not preferred in remote sensing. Other than the file format, the physical size of the sensor also plays a role. Larger sensors allow more light to enter to produce an image, therefore, allowing the coverage of a wide range of light (dynamic range) and improve the signal to noise ratio (Fellgett 1953; Crisp 2013). This allows for more information to be captured without image deterioration

1.2.4. Key points

The foregoing discussion, summarised in Fig. 1.2, shows that: 1) complex interactions between a number of factors might result in location and condition-specific relationships between DN and SSC. 2) The direction of the relationship (positive or negative) depends on the colour of suspended sediments in comparison to the bed colour (in addition to the absolute colour values of both). This is in turn dependent on the composition of the various variables mentioned within each parameter of the factor ‘River Physiography’. 3) The accuracy of estimating DN value is dependent on various external factors. These factors need to be considered to ensure that as much information as possible (in terms of accurate DN value of the subject of interest) is preserved.

Several of these have already been explored extensively in the literature (e.g. sun angle, cloud cover, depth) but others are less well known (relative colours of suspended sediment and bed) and while in general sensor specifications are known to influence images, no studies have directly compared DN-SSC relations developed using smartphone and drone-mounted sensors, both of which have the potential utility for citizen science

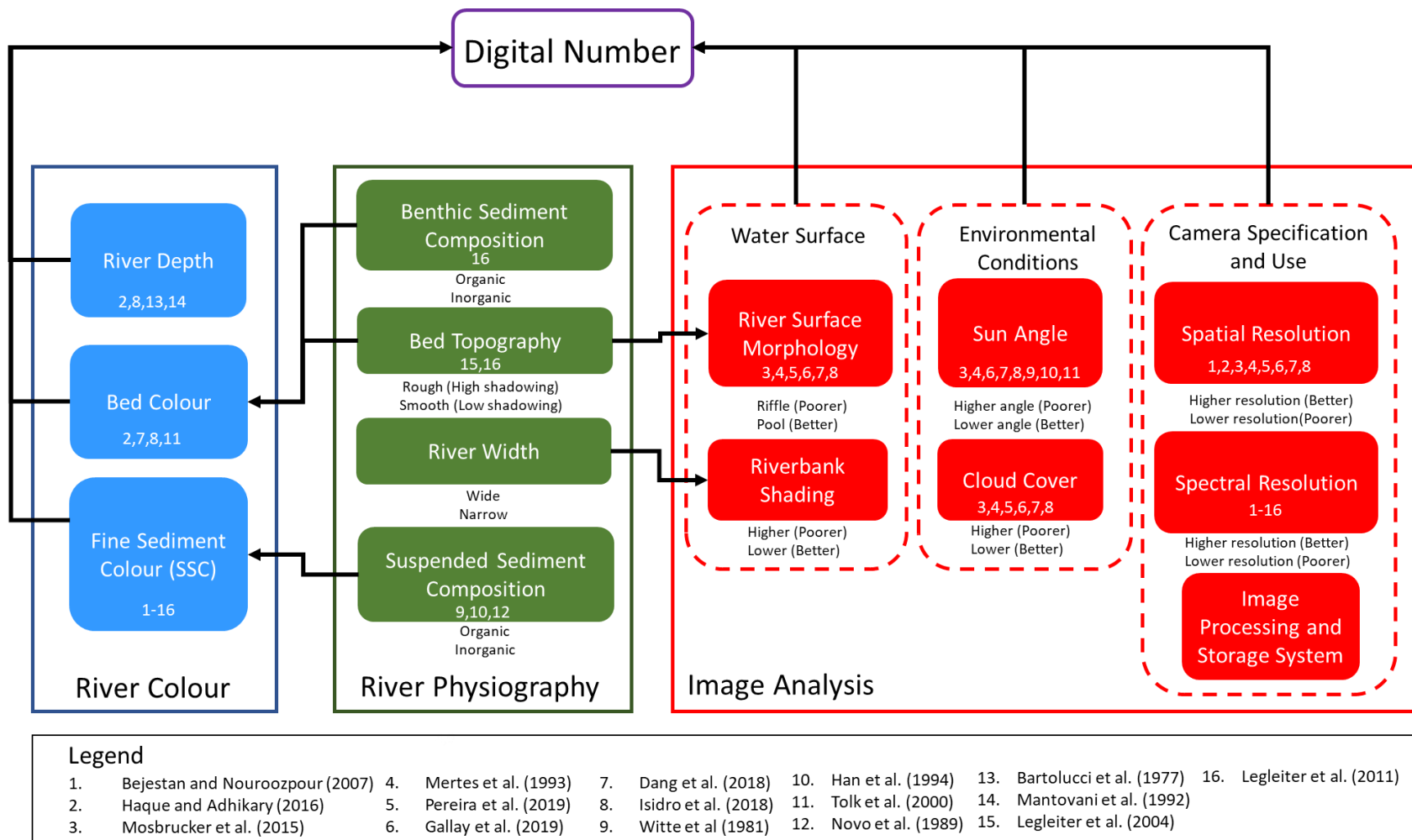


Fig. 1.2 Schematics of the factors that can influence the digital numbers in pixels in an image captured of the surface of a river. This schematic in affect represents the theoretical backgrounds that underpins this study. Numbers indicated in each box give examples of papers that have assessed respective factors. See text for details.

Table 1.1 List of research papers that use remote sensing to measure SSC in freshwater bodies. The table provides information on the camera sensors used, country, whether the studies use DN or reflectance values, the maximum SSC recorded, selected bands that have the strongest mode fit and the direction of trend line.

No.	Authors	Model	Country	DN/ Reflectance	Water Body (Lake/ River/ Lab)	Maximum SSC (mg/L)	Selected Band	Direction of trend line
1	Bejestan and Nouroozpour (2007)	Sony DSC-H1	Iran	DN	Lab	1000	Red, Green, Blue	Negative
2	Haque and Adhikary (2016)	Nikon D3000 DSLR and Canon S110	Bangladesh	DN	Lab	5500	Blue	Negative
3	Mosbrucker et al. (2015)	Nikon D800E	U.S.A	DN	River	7339	Blue	Negative
4	Mertes et al. (1993)	Landsat TM	Brazil (Field) U.S.A (Lab)	Reflectance	River, Lab	180 (Field) 207 (Lab)	Blue, Green, Red, NIR	Negative
5	Pereira et al. (2019)	RapidEye	Brazil	Reflectance	River	230	Green, NIR	Positive
6	Gallay et al. (2019)	MODIS	Venezuela Colombia	Reflectance	River	560	NIR	Positive
7	Dang et al. (2018)	Landsat TM/ETM+	Vietnam	Reflectance	River	400	Coastal aerosol, Blue, Green, Red, NIR	Positive

8	Isidro et al. (2018)	RapidEye, Pleades-1A, SPOT-6	Philippines	Reflectance	River	4251	Red	Positive
9	Witte et al. (1981)	Transmissio- meter	U.S.A	Reflectance	Lab	700	NIR	Positive
10	Han et al. (1994)	Spectroradio- meter	U.S.A	Reflectance	Lab	1000	(Red, NIR) response for chlorophyll-a	Positive
11	Tolk et al. (2000)	Spectroradio- meter	U.S.A	Reflectance	Lab	400	Red, NIR	Positive
12	Novo et al. (1989)	Spectroradio- meter	U.S.A	Reflectance	Lab	100	(White clay) Red, NIR (Red silt) Blue,Green	NA
13	Bartolucci et al. (1977)	Spectroradio- meter	U.S.A	Reflectance	River, Lake	99	Red	NA
14	Mantovani et al. (1992)	Spectroradio- meter	U.S.A	Reflectance	Lab	140	NA	(Negative) response to depth
15	Legleiter et al. (2004)	Spectroradio- meter	U.S.A	Reflectance	River	8	Red, Green	(Negative) response to depth
16	Legleiter et al. (2011)	Spectroradio- meter	U.S.A	Reflectance	River	108 (Cottonwo d) 161 (Rowe)	Blue, NIR	Negative

1.3. Problem statement and research gaps

There is already a considerable literature using remote sensing to assess different aspects of freshwater quality, including suspended sediment. However, many have focussed on larger rivers. There is a need to look at prospects for use in small rivers. Also, small streams and rivers tend to have shallower depths and accordingly, it is more likely that the bed is visible in aerial images. In turn this means that many of the factors than can impact DN come into play (e.g. bed colour relative to suspended material) in shallow streams, and inter-location differences may make transferability of regression models problematic. More generally, the majority of studies use reflectance rather than DN. Those that have used DN have often required complex image sequence to be taken at each location (e.g. of sky, water and of a white balance) which limit application in citizen science. Some authors have tested the use of individual consumer-grade cameras for quantifying changes in SSC and have found a strong fit between SSC and DN using these cameras (e.g. Bejestan and Nouroozpour (2007); Mosbrucker et al. (2015)). Haque and Adhikary (2016) conducted tank experiments to develop DN-SSC relationships using low costs cameras. However, in the paper they did not directly compare relations developed using images from respective cameras. None of these papers explicitly assessed the general transferability of the derived models between sites.

From the literature reviewed above (summarised in Table 1.1), it can be concluded that there are several research gaps that can be addressed in this study. 1) Whether robust estimates of SSC can be derived directly from DN, rather than reflectance, 2. whether DN values derived from smartphones and sensors in cheap, consumer drones can produce reliable estimates of SSC, and 3) How interactions between fine sediment and bed colour influence DN-SSC relations and, in turn, what this means for transferability of models in small streams where the bed is commonly visible. This thesis aims to address each of these three gaps.

1.4. Research Aims and Objectives

Suspended sediment is one of the key parameters that influence the health of river ecosystems. Thus, monitoring fine sediment is key to reducing the degradation of river ecosystems. This thesis aims to assess the potential application of low-cost cameras for monitoring suspended sediment through close-range remote sensing. The main objectives are:

1. Assess whether it is possible to estimate SSC from simple, uncalibrated DN values (rather than reflectance).
2. Assess the influence of different camera sensors and bed colour on the strength and statistical form of relationships between SSC and DN.
3. Assess whether it is possible to use DN to reliably predict spatial SSC across a river reach.

Objective 1 and 2 will be addressed in Chapter 3 through an experimental setup to produce a calibration model. Objective 3 will be addressed in Chapter 4 through drone flight test in the field to validate the calibrated models. In depth explanation in Chapter 2.3.

1.5. Structure of the thesis

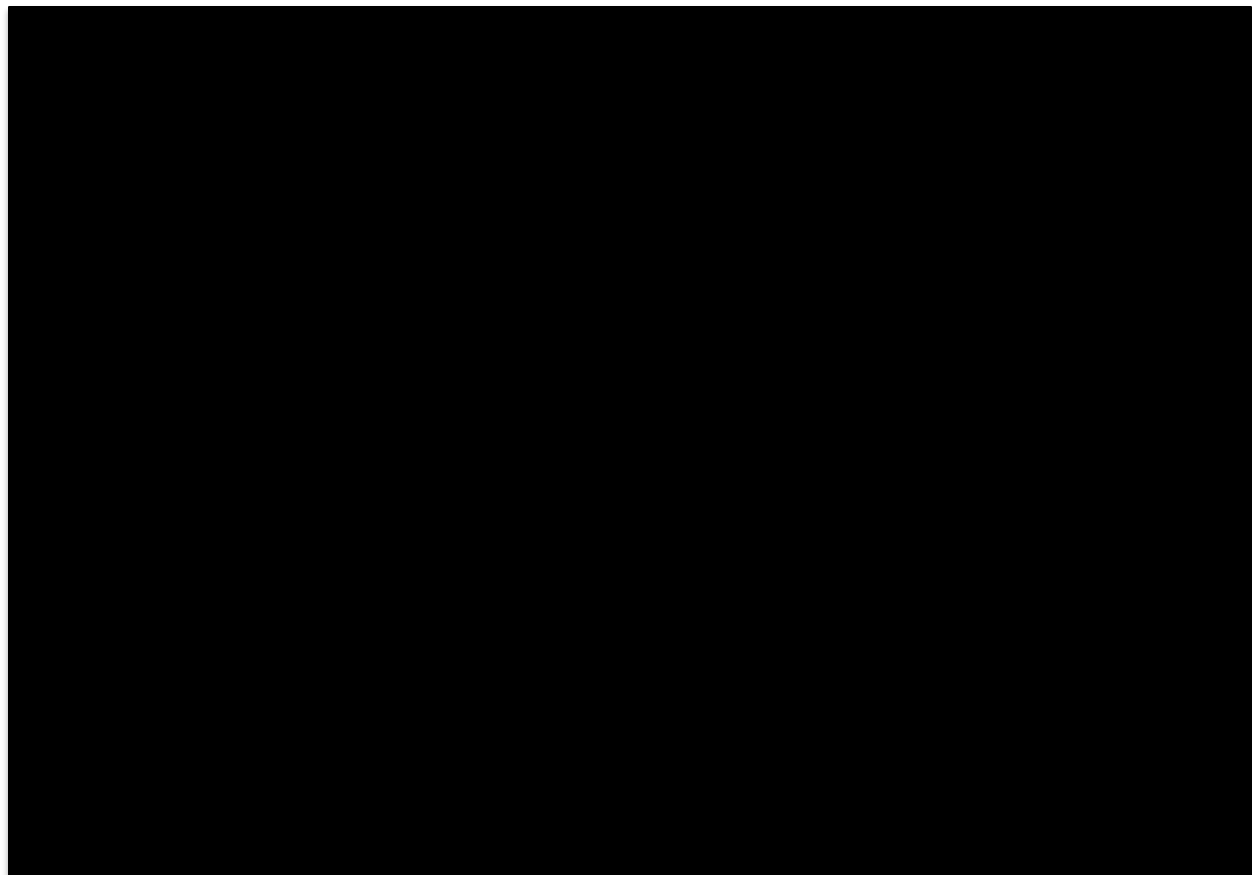
This thesis consists of five chapters: The present chapter provides a general introduction to the research. Chapter 2 provides information on the study area and gives an overview of the approaches used to address the objectives. Detailed methods are then given in respective chapters. The laboratory experiments used to address objective 1 and 2 are described in Chapter 3, while field tests used to address objective 3 are described in Chapter 4. Chapter 5 provides a summary of each chapter's results and discusses implications.

2. Chapter 2 Study Area and Methods

2.1. Langat Basin: rationale of study area selection

The Langat Basin straddles the states of Selangor and Negeri Sembilan on Peninsular Malaysia (latitude 2° 40' 12" N to 3° 16' 15" N and the longitude 101° 19' 20" E to 102° 1' 10" E). It

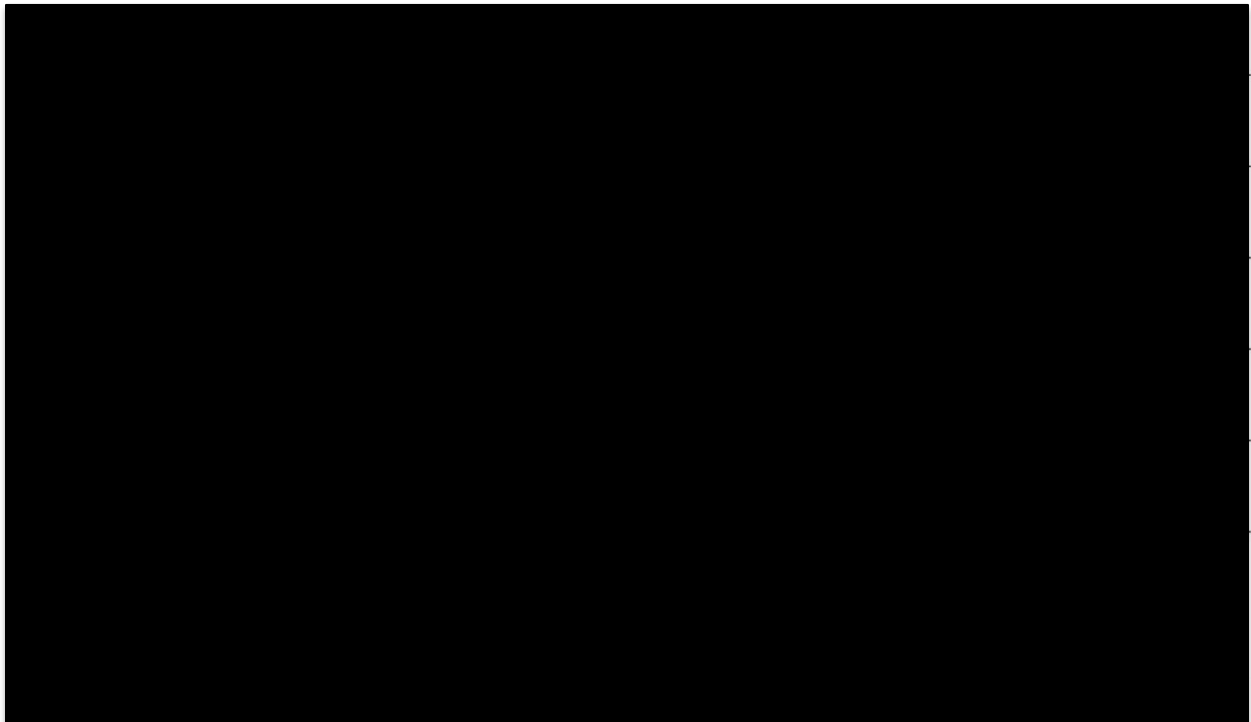
originates to the northeast of Kuala Lumpur and then skirts around the southern edge of Selangor; accordingly, it is one of the most populated and developed catchments in Malaysia [REDACTED]. The area of the basin is 2 140.6 km² and the main tributaries of the Langat River are the Semenyih River, Lui River and Beranang River. The study site within the study area [REDACTED] is located near the University of Nottingham Malaysia where one of the main tributaries (Semenyih River) is located less than 10km away from the campus (further details of exact location is stated in Chapter 4). This has allowed ease in logistics and data acquisition over a regular basis. The location of the river basin at one of the most populated areas in Malaysia has been the subject of interest of previous hydrological and remote sensing studies (Noorazuan et al. 2003; Idrus and Samad 2006; Ayub et al. 2009; Memarian et al. 2012; Basheer et al. 2017)



2.2. Characteristics of the Langat

2.2.1. Climate

The climate of the Langat Basin is greatly influenced by the moist monsoonal air streams. In particular, the southwest monsoon provides more precipitation to the region than the northeast monsoon where precipitation is obstructed by the Titiwangsa range (Suhaila et al. 2010). The climate is characterized by high humidity (between 80-88%), abundant rainfall and little variation in temperature throughout the year with an average of 26 to 32°C (Azhari et al. 2008). Long term data by Amirabadizadeh, Huang, and Lee (2015) indicates that the mean annual rainfall of the Langat River Basin is 1 994.1 mm with the highest recorded monthly rainfall at 327.1 mm, occurring in November; the lowest at 97.6 mm in June [REDACTED]. These two maximum and minimum precipitations occurred in the northeast monsoon and the southwest monsoon periods, respectively. While the mean annual maximum temperature [REDACTED] and minimum temperature [REDACTED] ranged from 31.6 to 33°C and 21.6 to 24.2°C respectively. Overall the study showed that climate change are expected to cause an upward trend of annual precipitation (from 12.6 to 17.1 mm/year) and an upward trend for the annual and seasonal maximum and minimum temperature range (from 3.5 to 4°C /century).



2.2.2. Geology and Soils

The mountainous region located north to northeast of the Langat Basin is part of the Titiwangsa range and has a bedrock layer composed of Permian igneous rocks and Pre-Devonian schist and phyllite of the Hawthornden Formation (Gobbett et al. 1973). Downstream of this region, the hilly areas in the Langat regions are made up of the Kenny Hill Formation and Kajang formation which is comprised of metamorphosed sandstone, shale, mudstone and schist from Middle Silurian to the Triassic period (Lee 2001; Leslie et al. 2020). On the coastal plains, the basin consists of thick quaternary alluvium deposits from the Paleocene through Holocene (Leslie et al. 2020). These layers reside in the low flatlands of the Simpang, Kempadang, Gula, and Beruas Formations that are identifiable due to their unconformable overlay eroded bedrock that grows younger and thicker towards the coast (Abd Manap et al. 2014).

Key soil units found in the region can be referred in Table 2.1. Each soil unit is further divided according to its dominant, and associated soil orders. The map shows that the majority of the soil type of the Langat Basin comes from the soil group A0108-2ab at roughly 50% located in the central area the Langat Basin. These soil group is dominated by Orthic Acrisols which has a clay rich subsoil. The next soil group is dominated by Ge55-3a and Od21-a each occupying roughly 20% of the basin located near the coast. Ge55-3a soil group is dominated by Eutric Gleysols which are soils that hold wetland water and are saturated in groundwater for long periods of time. Od21-a soil group is dominated by Dystic Histosols which are peat soils that comprise of incomplete decomposed plant remains. The last soil group is A090-2/3c which occupy roughly 12% of the basin located in the mountainous region where it also has a dominant Orthic Acrisols soil profile.

Table 2.1 Spatial distribution of soil features in the Langat River Basin (Islam et al. 2020).

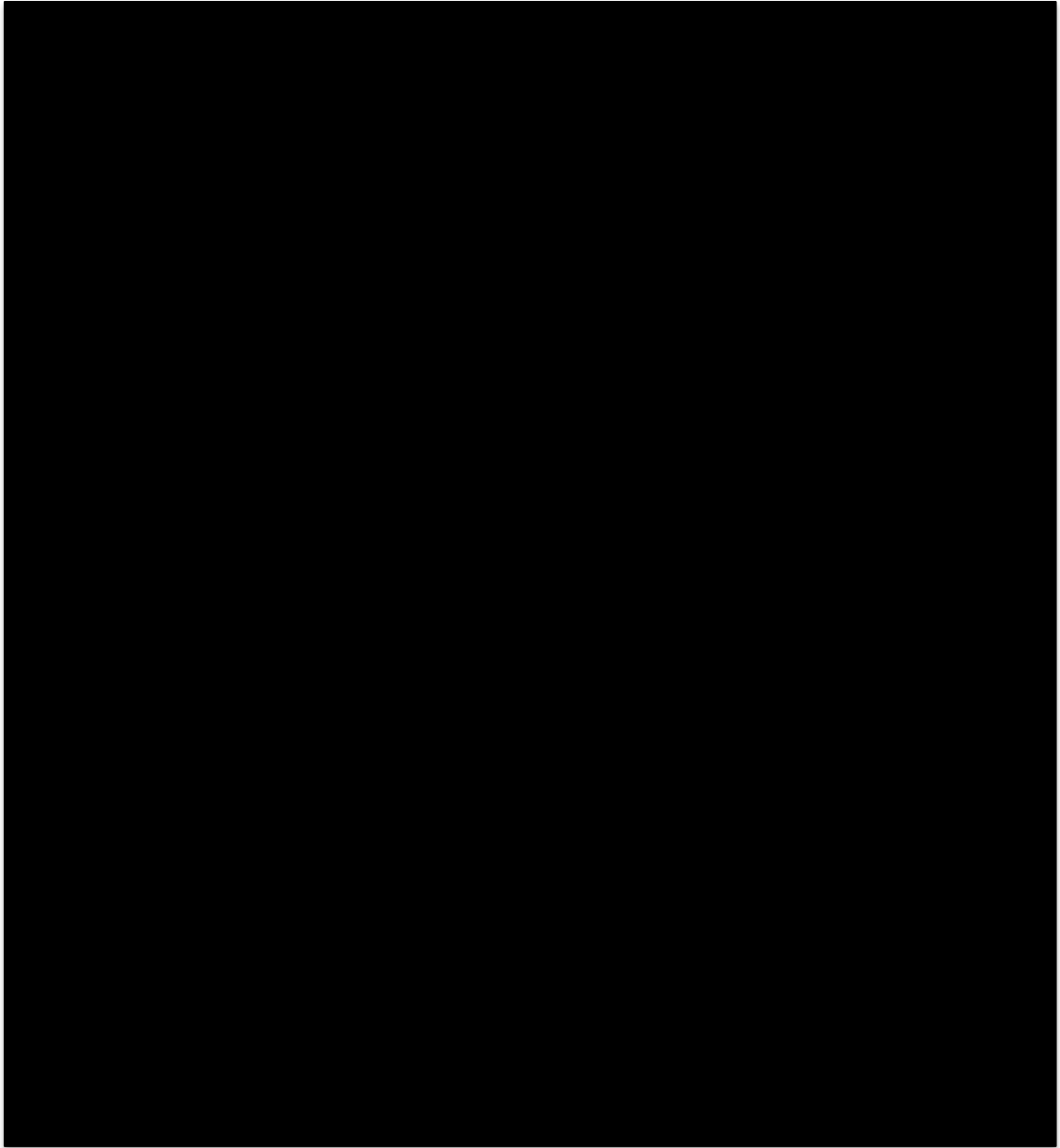
Soil mapping unit symbol	Soil unit	Soil group
A090-2/3c	Dominant soil	Orthic Acrisols
	First associated soil	Humic Acrisols
	Second associated soil	Dystric Cambisols
	Third associated soil	Lithosols
Ge55-3a	Dominant soil	Eutric Gleysols
	First associated soil	Gleyic Cambisols
	Second associate soil	Thionic Fluvisols
A0108-2ab	Dominant soil	Orthic Acrisols

	First associated soil	Ferric Acrisols
	Second associated soil	Dystric Nitosols
	Third associated soil	Gleyic Acrisols
	Forth associated soil	Chromic Vertisols
Od21-a	Dominant soil	Dystric Histosols
	First associated soil	Humic Gleysols
	Second associated soil	Thionic Fluvisols

2.2.3. Land use and Land cover

Land cover analysis of the Langat Basin by Islam et al. (2020) has shown that the basin is dominated by agricultural land, particularly by oil palm plantations and other permanent crops (39.25%). At least 25% of the area is occupied by forest, including swamp mangrove and the wetland forest. These forests and wetlands are mostly protected areas, serving as water catchment areas and conservation areas (Ekhuemelo et al. 2016; Widney et al. 2018). The urban settlements and associated non-agricultural areas make up approximately 20% of the basin.

Idrus and Samad (2006) conducted a study of the rate of land cover change in the Langat Basin between the years 1974-2001. The study showed that the percentage of urbanisation almost doubled from the year 1996 (7.85%) to 2001 (13.86%). Much of the Langat Basin was occupied by agriculture in the 1960s and 1970s occupying roughly 50% of the basin. The rapid land-use change from 1996 to 2001 was due to the development of an administrative centre now known as Putrajaya and Cyberjaya. This development paved the way for the acceleration of the conversion of agriculture areas into urban areas. Agricultural areas have shown a decline from 176 640 hectares in 1996 to 164 841 hectares in 2001 and continues to this day.



2.2.4. Hydrology

As mentioned above, the Langat Basin has experienced accelerated change, particularly in intensive agriculture and urbanisation which have led to marked changes in its river hydrology. There has been a significant increase in discharge in the Langat Basin over the last 30 years (Memarian et al. 2012). The study was conducted at the Langat River and Semenyih River. The study shows that the mean water discharge of the Langat River experienced a 77% increase while the Semenyih River experienced a 44% decrease.

2.2.5. Characteristics of the study site

The study site is located at a confluence between the Semenyih River and the Lalang River which is a 2nd and 1st order river respectively. The interaction between the climate, geology and soils, land use and land cover, and hydrology as mentioned in the previous sections are critical in determining the influence of various factors mentioned in Fig. 1.2 but most importantly the influence of bed colour on the estimation of SSC. More details on the study site are discussed in Chapter 3.

To demonstrate, the study site of this thesis is located within the soil group A0108-2ab which is dominated by a clay rich subsoil. The Lalang River has a river bed that is characterised with the mentioned soil group which gives off a light-brown bed colour. The deposition of fine sediment is further amplified by large scale agricultural activities upstream of the catchment which results in an uncontrolled erosion rate. On the other hand, the Semenyih River is a 2nd order river and does not show the characteristics of this soil group, instead has a sand and gravel bed which gives off a dark-brown bed colour. This is due to the higher water velocity of 0.5 m/s as compared to the Lalang River of 0.15 m/s which transports fine sediment downstream, depositing larger sand/gravel sediment particles. Furthermore, the upstream catchment of the Semenyih River is a protected forest reserve maintaining a lower erosion rate than the Lalang River. The interaction between the natural and anthropogenic characteristics resulted in a change in bed and water colour between the two rivers despite occupying the same catchment. These interactions also influence other factors such as channel depth and suspended sediment type which are discussed in Chapter 4.4.2.

2.3. Methodological framework

The theoretical background related to the signature and detection of material present in water (section 1.2.3) raised a number of issues that potentially affect estimates of SSC derived directly from DN values. The methods adopted for this work were designed to address some of these issues, and accordingly the overall framework blended approaches used in previous work and expanded certain areas to explore them in greater depth. In particular, this thesis builds upon the methods (and underlying theory) of Mosbrucker et al. (2015) and Haque and Adhikary (2016). The former was a study of the applicability of using consumer-grade cameras to estimate SSC using DN values from images taken from bridge vantage points. Their field site was deep so the bed was not visible, therefore some of the complications related to shallows streams were not considered. Their general approach to deriving DN and calibrating values from images was used here, but adopted in both laboratory experiments and field tests. These experiments followed Haque and Adhikary (2016) methodologically, but unlike these authors data were used to make statistical comparisons of the shape and quality of models fitted to DN v SSC. Unlike either of these studies, the present work also involved developing and validating calibration equations in the field using drone-surveys. Thus, the methodological framework blended field and laboratory studies and included using drone images to produce SSC maps of river reaches. In addition, unlike previous work flexible, non-linear models (Generalised Additive Models (GAMs)) were used to assess and compare relations between cameras and across different types of bed conditions. Advantages of GAMs are discussed further below.

The methodological framework of this thesis is represented schematically in Figure 2.5. It involves 1) obtaining remote sensing imagery at controlled SSCs in the laboratory, with different experiments designed to assess the influence of bed colour and sensor, 2) undertaking drone flights and developing field calibrations from images, to produce (3) a final orthomosaic that shows SSC in a small, shallow river. Methods specific to each objective are detailed in respective chapters, as illustrated in Fig. 2.5. Chapter 3 presents the methods and results of lab work designed to address Objective 1 and 2. It will explore the influence of multiple parameters (bed colour and camera sensor) that may affect the strength and nature of the relationship between SSC and DN. Chapter 4 details the field studies using the drone. It sets out how images were processed in order to develop a field calibration relationship, and tests (validates) this using empirical SSC data for the site. The final product is a map showing fine-scale (cm resolution) spatial variation in SSC across the reach, something which would be difficult and/or expensive to achieve using traditional SSC monitoring approaches (i.e. in-situ sensors and satellite-based remote sensing).

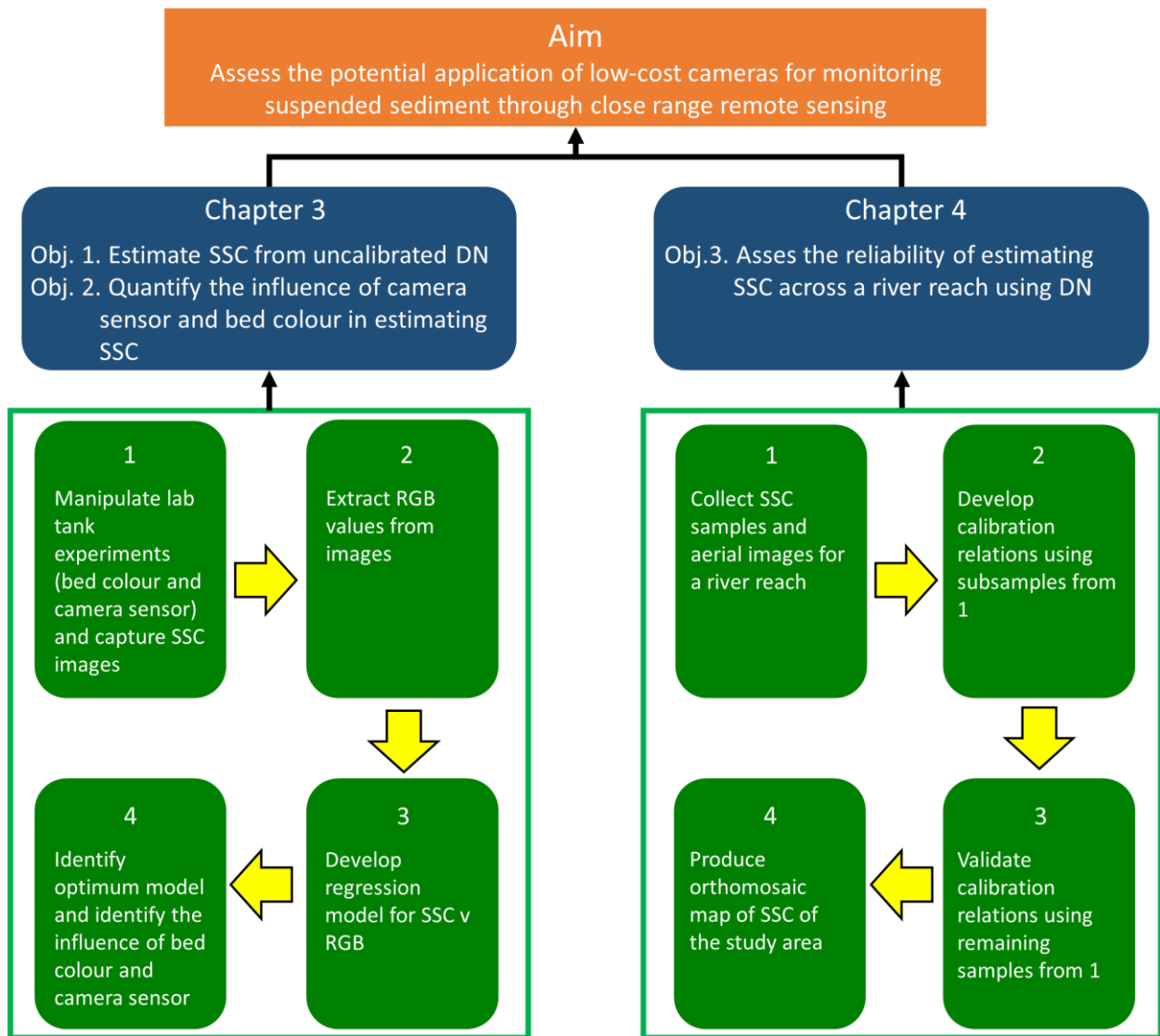


Fig. 2.5 Research framework used in this thesis.

3. Chapter 3 Close Range Remote Sensing of Suspended Sediment in Tropical Rivers: Determination of key drivers using laboratory experiments

3.1. Introduction

Rivers and streams around the world are threatened by a range of stressors (Dudgeon et al. 2006; Ormerod et al. 2010). While some new stressors have emerged quite recently (Reid et al. 2019), others have remained persistent and widespread. One of the most persistent and globally pervasive threats to aquatic ecosystems comes from elevated concentrations of fine sediment (Owens et al. 2005). The impacts of changes in river fine sediment loads have long been recognized (Lal 1985), and a substantial literature now exists on causal processes and transport mechanisms (Wenger et al. 2017, Vercruyssen and Grabowski 2019), and the ecological impacts of fine sediment both in suspension and once deposited on the bed (Wood and Armitage 1997; Buendia et al. 2014, Wenger et al. 2012). Changes in the amount of fine material transported by rivers have implications for coastal regions that impact the flow of nutrients (Noe and Hupp 2009) and changes the deposition-erosion dynamic that governs the size of coastal ecosystems such as mangroves and wetlands (Caldwell and Edmonds 2014). As a result, coastal regions that experiences increase fine sediment also experiences heavy metal concentrations due to the cohesive and flocculating nature of fine sediment (Qian et al. 2015). High concentrations of heavy metals then enter the nutrient cycle in coastal food webs. Areas that experience deficit fine sediment have reduced nutrient flow such as nitrogen and phosphorus (Noe and Hupp 2009) but most concerning, experiences loss in coastal areas due to an increase in coastal erosion and a decrease in sediment deposition (Aiello et al. 2013).

As discussed in Chapter 1.2 and illustrated in Fig. 1.2, published tests of simple direct methods remain limited but so far have suggested that DN has potential for river applications. For instance, Mosbrucker et al. (2015) developed linear equations that were able to predict, SSC from DN with a mean error of 10%. Bejestan and Nouroozpour (2007) used laboratory tests to generate values of SSC from DN values. While these studies show the potential for this approach, they were one-dimensional in that they showed the existence of relationships in a particular set of circumstances (single rivers, single sensor), and used a narrow range of SSC conditions with the exception of Haque and Adhikary (2016) which used two different sensors but the differences from the results were not discussed in detail. Thus, there remains the need to assess whether SSC

can be predicted from DN using ‘generic’ transferable equations, or whether specific ones are needed for each application (reflecting the sensor being used in local conditions). This experiment addresses objective 1 and objective 2 of the thesis as mentioned in Chapter 1.3 and 2.3.

Objective 1. Assess whether it is possible to estimate SSC from simple, uncalibrated DN (i.e. rather than reflectance).

Objective 2. Assess the influence of different camera sensors and bed colour on the strength and statistical form of relationships between SSC and DN.

To fully realise the stated objectives, there are three research questions needed to be answered:

1. What are/is the statistically best colour channels to estimate SSC?
2. Do different cameras sensors affect the quality of estimation? and
3. Does the change in bed colour affect the estimation of SSC?

3.2. Methods

3.2.1 Experimental setup

SSC-DN relations were developed from a series of laboratory tank experiments (Fig. 3.1). The tank was 0.7 m long, 0.3 m wide and 0.5 m deep; it was open at the top and had white walls and base. All experiments were conducted in a closed room, under fluorescent ceiling lights with no natural lighting.

For each experiment, the tank was filled with water to a depth of 0.3 m. A sediment of $<56\mu\text{m}$ was added incrementally in known weights to the water to produce a series of controlled suspended sediment concentrations extending from 0 to 2.5 g/L. This range was set to reflect SSCs in the river from which the sediment was collected (Langat River, Selangor, Malaysia; min 0.0028 g/L and max 2.3123 g/L) and whose bed colours were mimicked (Fig. 3.2).

For each concentration, four photographs (JPEG) looking down at an angle 45° onto the tank were taken using two different cameras – a commercial drone camera (DJI Mavic Pro) and a smartphone camera (Vivo V9) (Table 3.1). The specific camera angle is set to reduce glare and reduce reflection from the camera setup and follows Mosbrucker et al. (2015). Water was agitated

immediately before each image was taken, to suspend sediment and mix it as evenly as possible within the water volume. The cameras were set to identical image capture settings as per Table 3.1 where a Kodak white reference card was used to ensure that the images were set to true white. Photographs were taken from 0.5 m above the water surface. Before and after the experiment a photograph was taken of the aforementioned white balance with each camera. This was to ensure that any changes in the ambient lighting before and after the experiment could be corrected. A two-tailed paired t-test was conducted for the respective R, G and B from the images of the white balance before and after the experiment. The test showed that no significant change in the RGB values ($P < 0.001$, $df = 520$ 198) occurred before and after the experiment.

A 0.3 m x 0.3 m commercial non-polished ceramic tile was placed on the bed of the tank. In the first set of experiments, this tile was painted with a grey-brown colour (Nippon Paint 3616 Pebble Walk) to represent light riverbed material. A series ($n = 80$) of images were taken for each camera-SSC combination. Experiments were then repeated with a different tile colour (Anchor Spray No. 19 Anti-Rust Primer) which represents the more brown-red sediments found in the Langat. For the red-brown tile, only 30 experiments ($n = 30$) were undertaken, covering the same SSC range (0-2.5g/L). The same cameras and camera settings were used for the red-brown tile. Fig. 3.2 shows the two tiles representing different bed colours where the first colour is grey-brown while the other is brown-red. Experimental treatments using the left tile (grey-brown) will be referred to as Grey tile while treatments using the right tile (brown-red) will be referred to as the Brown tile for simplicity.

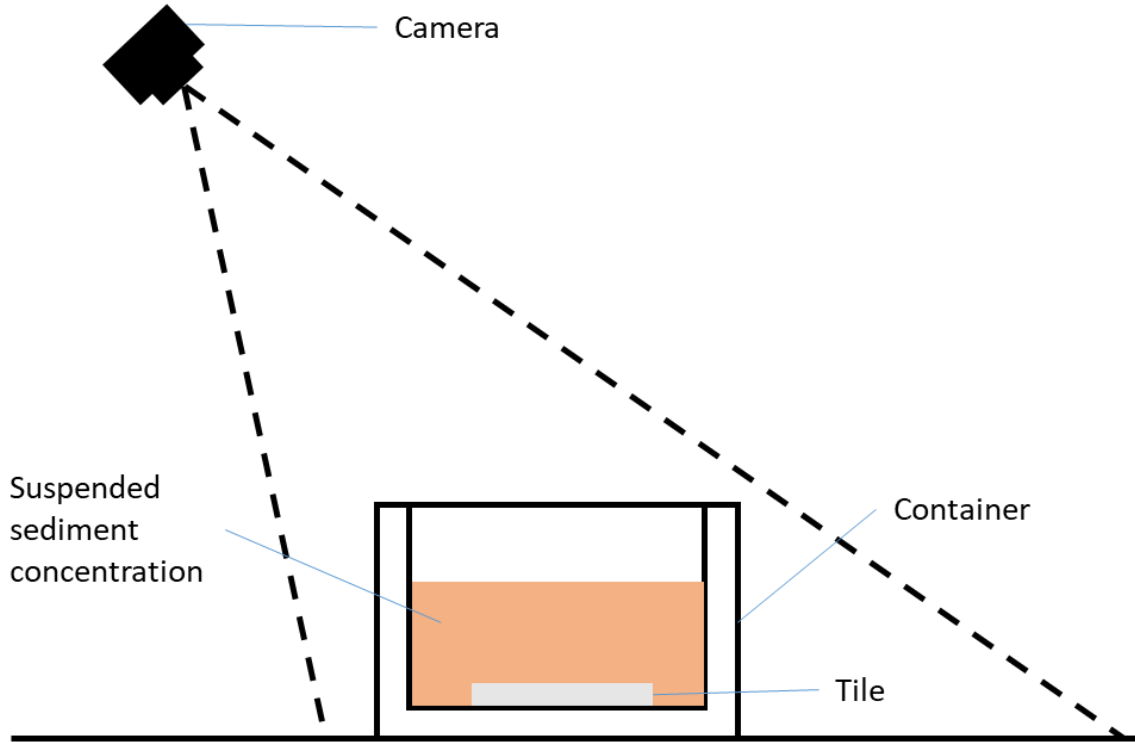


Fig. 3.1 Setup of the laboratory experiments indicating the position and angle (45°) of the camera relative to the water filled tank and bed tile.

Table 3.1 Camera specifications and settings of the drone (DJI Mavic Pro) and phone (Vivo V9). There was no available information on the sensor size of the Vivo V9 rear camera. Digital white balance is set according to a physical white balance card before the experiment began.

	DJI Mavic Pro	Vivo V9 (rear camera)
Sensor	Complementary Metal Oxide Semiconductor (CMOS)	CMOS
Sensor size	6.2 x 4.6 mm ($1/2.3''$)	N/A
Pixel Resolution	12 MP	16 MP
ISO	200	200
Exposure time	1/50	1/50
White Balance	Sunny	Sunny

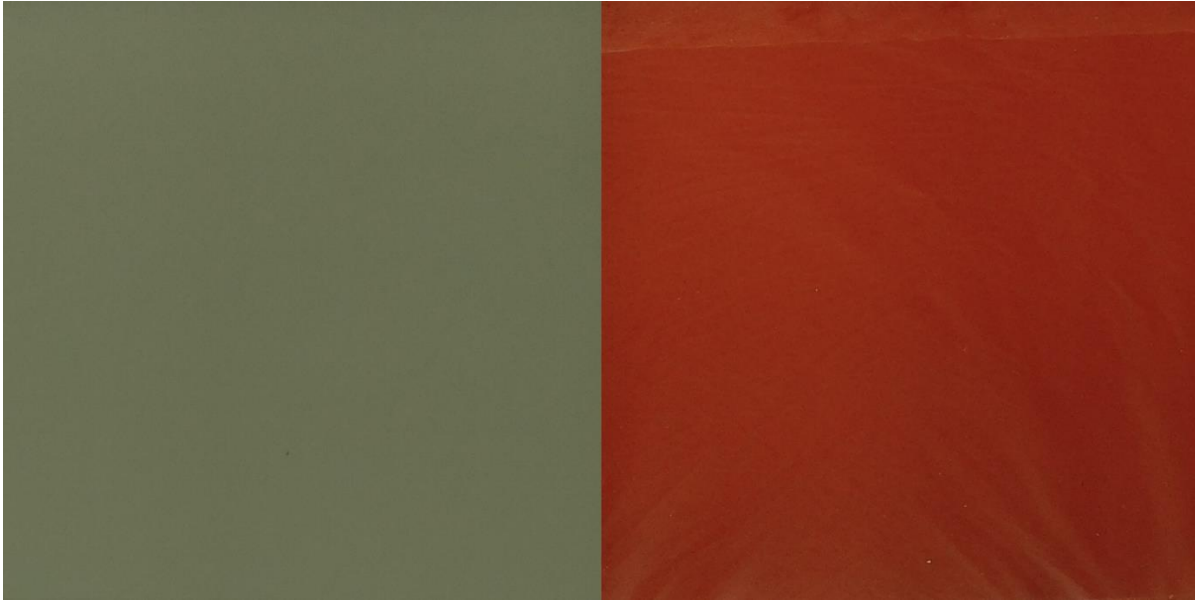


Fig. 3.2 Different tiles used to simulate effects of bed colour on estimates of SSC. These images are from the painted tiles that are immersed in potable water (0.0 g/L) and then cropped.

3.2.2 Data processing and statistical analysis

All data processing and statistical analysis were conducted using Microsoft Excel 2008 and R Studio 4.0.2 (R Core Team 2020) using the ‘raster’ (v3.3-13; Robert 2020), ‘plotrix’ (Lemon 2006) and ‘rgdal’ (v1.5-16; Bivand et al. 2020) packages. The photographs were cropped to include only the central part of each tile in the image for analysis. This cropping ensured that the area used for analysis (25cmx25cm) was not affected by shadows from the tank sides.

DN values for each pixel were extracted for Red, Green, and Blue (R, G, and B) channels for each image crop. For each RGB colour channel from each image, the mean DN values were calculated. The mean DN value was used based on a preliminary study that compared the fits for the mean, median, maximum, and minimum DN values. The preliminary study found that the mean and median DN values displayed the strongest and most consistent relationship to SSC with both having deviance explained of 96%. The minimum and maximum values had the weakest relationship with deviance explained of 87% and 74% respectively.

The relationships between SSC and mean DN were initially explored for each ‘tile colour-camera-colour channel’ combination using x-y scatter plots. The main method of identifying a suitable statistical relationship was by fitting a Generalised Additive Model (GAM). GAM is a generalized linear model where the linear response variable is linearly dependent on unknown smooth functions of some predictor variables (Nisbet et al. 2018). This allows the GAM to produce

a flexible model that find the best ‘shape’ without imposing a fix or assumed response (Nisbet et al. 2018). From the GAM models produced for every combination, the fit of the modelled relationships was quantified using model p -value, R^2 , and deviance explained, while the relative fit between different models was assessed using Bayesian Information Criterion (BIC) values. BIC is a quantitative way to represent information loss in a model, with smaller values representing a better fit (i.e. less information loss). One model is considered better than another if its BIC value is smaller by a value 2 BIC units (Kass and Raftery 1995).

3.3 Results

3.3.1 Thresholds for measurement of Suspended Sediment Concentrations (SSC) using Red, Green and Blue Digital Number (DN) values in camera images

Fig. 3.3 is the SSC-DN data fitted to GAMs. All the models gave a $P < 0.001$ with the Grey tile having a deviance explained between 60% and 80% while the Brown tile having a deviance explained between 80% and 30% with varying smoothness indicated by the estimated degrees of freedom (edf). The larger the edf, the more flexible and more complex the model is. The GAMs show that there is a statistically distinct trend between tile colour with the Grey tile having a negative relationship while the Brown tile having a positive relationship. Though GAM fits are statistically significant ($P < 0.001$) it is evident that in many cases there is a systematic pattern in the error around models with high scattering at high SSCs.

Generally, the relationship is much stronger at lower SSC and as SSC increases the estimation breaks down at a certain point. For instance, the Grey-Drone-R/G/B combinations breakdown when $SSC > 0.5$ g/L. The inclusion of this scatter prevents the accurate estimation of SSC, as such the threshold must be identified, and a new model must be fitted to the truncated dataset accordingly. The presence of a threshold is not as evident for models from the Brown tiles. The models for the Brown-Drone-Red, Brown-Phone-Red and Brown-Phone-Green combination (highlighted in red) can be argued to reasonably show relations across the complete range of SSC.

BIC values can be used to quantitatively assess (aided by visual interpretation) whether the Brown tile models are accepted for subsequent analysis or would require truncation like the Grey tile models. Models of low BIC value of differences < 2 BIC units indicate that the models are statistically the strongest model that have the least amount of information loss at the same time has the simplest models. The Brown-Drone-Red, Brown-Phone-Red, and Brown-Phone-Green was chosen to not have this vertical wall based on the fact that they have the smallest BIC

value (44.07, 42.20, 45.91 respectively) among all other models while at the same time, there is a fair amount of distribution of DN that can be interpreted to predict SSC value. Hence, these selected models will not undergo truncation like the other models and will be used in subsequent analysis.

The truncation is dependent on a quantitative analysis on the location of the threshold. A visual estimation was first required to estimate the breakpoint where DN remains constant as SSC increases for each SSC-DN combination. GAMs were iteratively fitted from low SSC values until a bit over the estimated breakpoint value. For each iteration, the BIC value is recorded and plotted against the sample size. The breakpoint is identified when there is a sudden change in the BIC value trend. For example, the Grey tile has 80 samples size of SSCs ranging from 0.0-2.5 g/L, visual estimation of the breakpoint occurs when SSC is at 0.5 g/L. A GAM was iteratively produced from 0.0-0.75 g/L with each BIC value recorded. This process is repeated for every SSC-DN combination.

Appendix 1 is the plotted points between the sample size and BIC value for every SSC-DN combination. The points in red are the BIC value that occurs before a large gap and is indicative of a breakpoint presented. The breakpoint for each SSC-DN combination is presented in Table 3.2. The results show that across different SSC-DN combination, the blue channel has the lowest SSC threshold followed by the green and red colour channel. The highest SSC threshold was from the Grey-Phone-Red combination at 0.95 g/L while the lowest SSC threshold was from the Brown-Phone-Blue combination at 0.25 g/L. These thresholds indicate the maximum SSC above which DN values cannot be reliably used to differentiate higher SSCs.

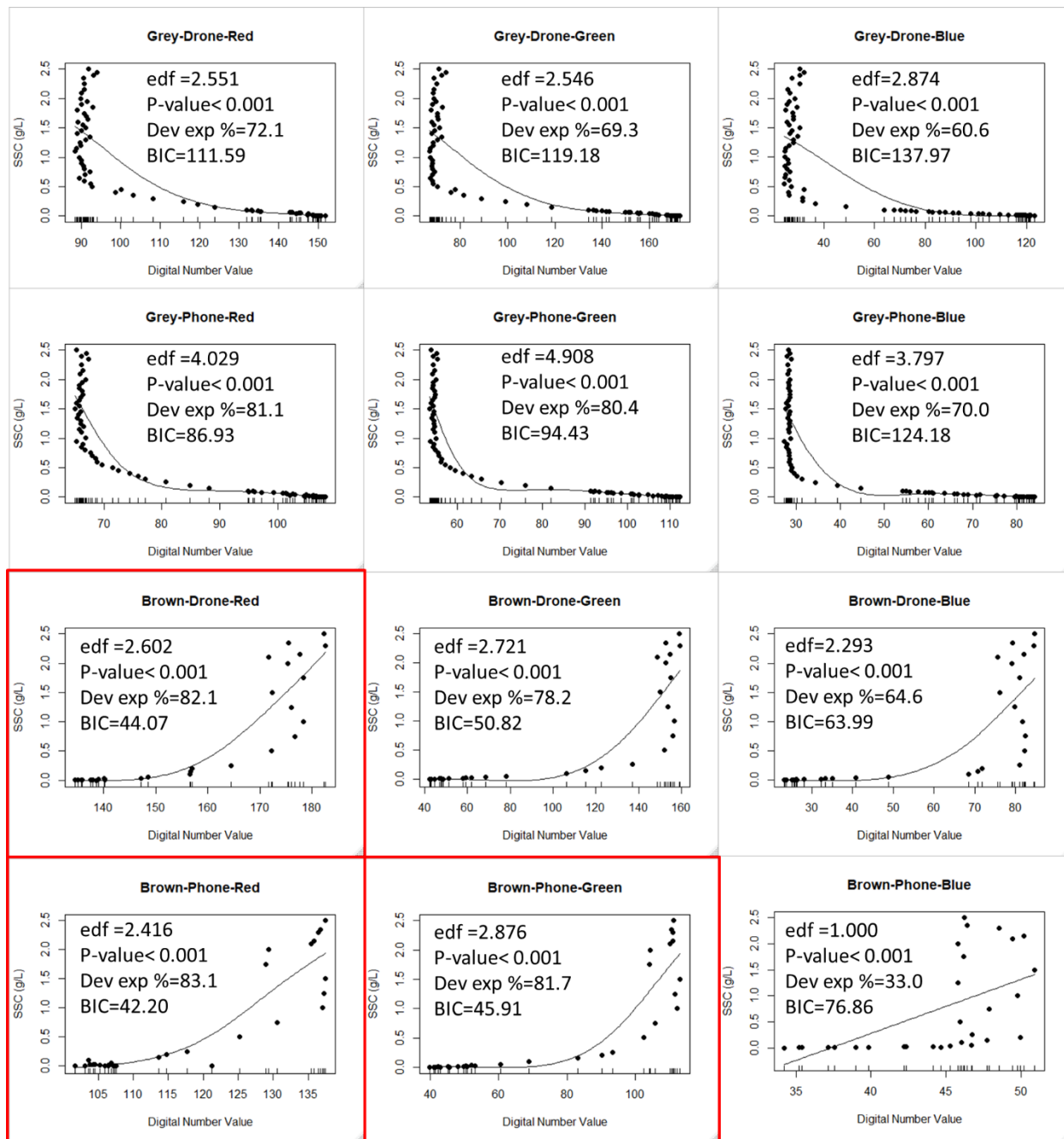


Fig. 3.3 GAMs for the SSC-DN combinations organised based on the ‘tile colour-camera-colour channel’.

Table 3.2. Threshold for each SSC-DN combination indicated by the largest gap in BIC value.

SSC-DN combination	SSC threshold (g/L)
Grey-Drone-Red	0.40
Grey-Drone-Green	0.40
Grey-Drone-Blue	0.25
Grey-Phone-Red	0.95
Grey-Phone-Green	0.60
Grey-Phone-Blue	0.30
Brown-Drone-Green	0.50
Brown-Drone-Blue	0.20
Brown-Phone-Blue	0.25

All truncated datasets were fitted to GAMs as seen in Fig. 3.4. along with the models that did not require truncation (highlighted in red). Table 3.3 is a summary statistic for each SSC-DN combination; Grey tile for the RGB of the phone and drone has an R^2 of >0.98 , indicating that the model explains more than 98% of all the variability of the response data around its mean. In respect to the Grey tile, the strongest model is the blue channel for the phone with $BIC = -295$ and green channel for the drone with $BIC = -332$; the model fits for the Brown tile for the blue channel for both cameras has an R^2 of >0.8 where the blue channel has the strongest BIC value of -83 for the phone and -93 for the drone.

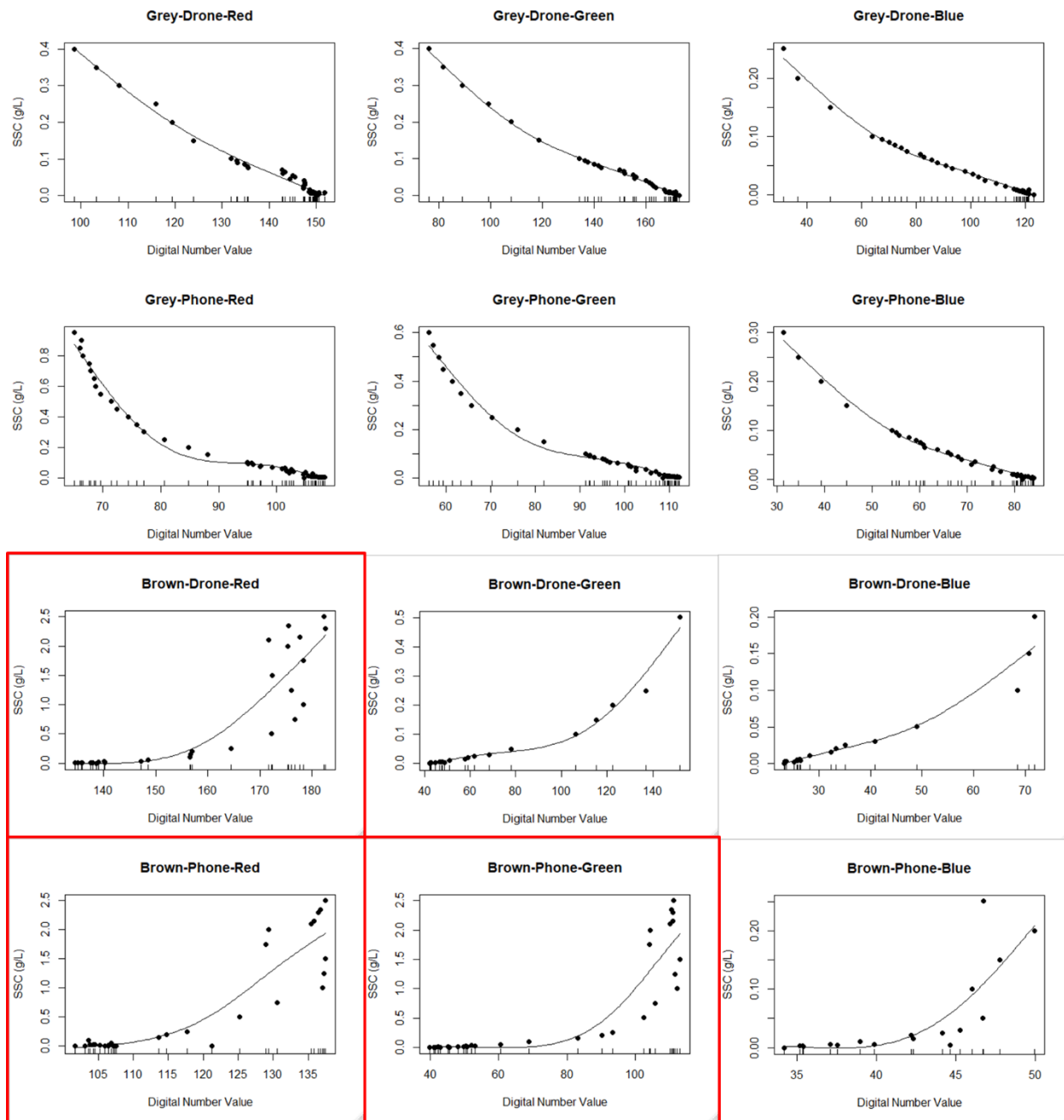


Fig. 3.4 GAM functions between Digital Number (DN) values of the Red, Green and Blue colour channel and Suspended Sediment Concentration (SSC) organised based on ‘tile colour-camera-colour channel’.

Table 3.3 Generalised Additive Models a) Grey tile and b) Brown tile for the RGB channel of each camera with their respective BIC, R², p-value, deviance explained % and edf. The strongest model is indicated by the BIC value labelled with *.

a)

Grey tile	Drone			Phone		
Channel	Red	Green	Blue	Red	Green	Blue
BIC	-248.87	-332.16*	-298.21	-204.84	-235.39	-295.67*
R ²	0.988	0.999	0.994	0.989	0.990	0.995
Dev exp %	98.9	99.8	99.4	98.9	99.1	99.5
p-value	< 0.001	< 0.001	< 0.001	< 0.001	< 0.001	< 0.001
edf	2.77	2.99	2.97	2.99	2.98	2.97

b)

Brown tile	Drone			Phone		
Channel	Red	Green	Blue	Red	Green	Blue
BIC	44.07	-36.02	-93.04*	42.20	45.91	-83.91*
R ²	0.804	0.916	0.967	0.816	0.816	0.928
Dev exp %	82.1	92.8	97.2	83.1	81.7	93.8
p-value	<0.001	<0.001	<0.001	<0.001	<0.001	<0.001
edf	2.60	2.83	2.80	2.42	2.88	2.23

3.3.2 Influence of camera type on estimated Suspended Sediment Concentrations using Digital Numbers from camera images

Fig. 3.4 shows that the overall DN values for the RGB of the drone camera has a slightly wider range than the phone for both tiles. The Grey-Drone has a DN range difference of 144, while the Grey-Phone has a difference of 83; Brown-Drone has a difference of 160, while the Brown-Phone has a difference of 103. The chi-squared test has shown that the differences in the range are statistically significant with a $P < 0.001$, $df=1$. Furthermore, the maximum SSC for the phone

camera is consistently higher than the drone camera across tile colour. E.g. the Grey-Drone-Red model has a maximum SSC of 0.4 g/L while the Grey-Phone-Red model has a maximum SSC of 0.95 g/L.

3.3.3 Influence of riverbed colour on estimated Suspended Sediment Concentrations using Digital Numbers from camera images

The direction of the trend line in Fig. 3.3 (positive or negative) indicates different relations between DN and SSC when bed colour differs. On the Grey tile, when the bed colour is lighter than the sediment, there is a negative direction and the trend appears to be exponential but in actuality, there is a wide range of SSCs at low DN values as discussed previously. On the Brown tile, when the bed colour is darker than the sediment colour, the slope is in the opposite direction and in most cases with scattering in DN at high SSCs. The only possible relations to exist across the whole range comes from the Brown-Drone-R, Brown-Phone-R/G colour channel, where there is no clear breakpoint that marks the breakdown in the relationship.

The direction of the relationship seen from the truncated data in Fig. 3.4 is that the Grey tile has a negative direction while the Brown tile has a positive direction. The overall range of DN values between the Brown tile is much wider than the Grey. The Grey-Drone has a DN range difference of 144, while the Brown-Drone has a difference of 160; Grey-Phone has a difference of 83, while the Brown-Phone has a difference of 103. Chi-squared test shows that these differences in range between tiles are statistically significant ($P < 0.05$, $df=1$). Both bed colours provide a good predictive model ($R^2 > 0.8$) as seen in Table 3.3.

3.4 Discussion

3.4.1 Potential of close-range remote sensing for monitoring suspended sediments in tropical streams and rivers

Close-range remote sensing has the potential in monitoring suspended sediments in smaller streams than satellite imagery and at a much greater spatial resolution (Mosbrucker et al. 2015). This technology may prove particularly beneficial in tropical environments where, first- to third-order streams are responsible for transporting high volumes of sediments into downstream river networks (Chappell et al. 2004) yet are typically too small for satellite remote sensing. The basic principles of extracting information on fine sediment from camera images are well established, and previous studies have shown that it is possible to estimate both water turbidity (Vogt and Vogt 2016) and suspended sediment concentration in lentic and lotic systems (Bejestan and

Nouroozpour 2007; Haque and Adhikary 2016). The laboratory tests reported here provide further evidence that that SSC can be predicted from DN values with confidence (i.e. significant models with high R^2), but they also indicate that 1) relationships may not be transferrable between rivers or sites where bed material differs in colour with respect to materials in suspension, 2) different camera sensors yield different calibration coefficients, and 3) in most cases, there is an upper SSC limit above which camera images are not able to differentiate further increases in SSC. These conclusions have implications for the use of digital photography for routine monitoring of suspended sediments and its utility in citizen science, as discussed below.

3.4.2 Thresholds for monitoring of SSC using DN values

The breakdown of the relationship between SSC and DN values has not been reported in the three studies that existed for close-range remote sensing for monitoring SSC through DN. The lab experiments indicate a threshold SSC value above which DN may not be able to distinguish further increases in SSC. Mosbrucker et al. (2015) used field data SSC values ranging from 0.25 - 7.3 g/L to produce a calibration relationship. The trend line produced was logarithmic (base 10) with a negative relationship. Haque and Adhikary (2016) conducted laboratory tests with SSC values ranging from 0-0.5 g/L. The trend line produced was linear with a negative relationship. And finally, Bejestan and Nouroozpour (2007) conducted laboratory tests with SSC value ranging from 0-0.1 g/L. The trend line produced was a quadratic equation with a negative relationship. None of these studies indicate a breakdown when SSC increases; such a breakdown might have been expected in Mosbrucker et al. (2015) as the maximum range of SSC in their study were three times higher than this current study. The breakdown is suspected to be a result of digital artefacts from the images. The digital artefacts mentioned could be a result of dark areas (cause by shadows) within the photos that conceal DN. Hence, a simple digital image processing was conducted on the image JPEG file by digitally increasing the exposure of the images and replotting the SSC-DN scatterplot. The results showed that the breakdown remained. Thus, interference from the image processors of the camera was ruled out. Future experiments could be replicated using images stored in raw as the preservation of image quality from this file format may remove the artefact. It is important to note that some SSC-DN combination of the Brown tile (red and green colour channel) shows no evident threshold and as such was not truncated as compared to the Grey tile. These models that were not truncated allowed for a much higher SSC coverage. E.g. the highest SSC for the truncated data is 0.95 g/L, while the non-truncated data goes up to 2.5

g/L. This can be used to affirm that the threshold is not likely an experimental artefact and that the presence of a threshold is influenced by the “Darkness” or “Lightness” of bed colour.

The most likely explanation for the breakpoint in our data is that DN values upon increasing SSC indicate that the maximum colour in the tank has been achieved (ratio of fine sediment colour is higher than the ratio of bed colour). Thus, any increments of suspended sediment can no longer change the overall colour of the image. Models that were not truncated simply has not reached its maximum colour. Applying these finding in the field, calibration models derived from the field that have a light bed colour (at least that of similar in colour to the Grey tile), the models would expect to only predict SSC at a drastically lower range than in areas that have a darker bed colour similar to the Brown tile. Despite the lack of ability for DN to estimate specific SSC above certain threshold for some situations, this approach can be used to test whether SSC exceeds particular levels. Thus, it can be used to assess if water sources meet water quality standards. According to the National Water Quality Standards of Malaysia, river water with Total Suspended Solids (TSS) higher than 3.0 g/L would be classified as Class 5 (Poorest water quality class) (National Water Quality Standards of Malaysia 2019) which is well below the threshold. This indicates that close-range remote sensing using smartphone or drone cameras can potentially be used to assign water quality classes based on SSC to Malaysian streams and rivers through cross calibrations of SSC v TSS.

3.4.3 Influence of colour band on DN values

The strongest fit for the colour channel was the green and blue channel. This conforms to Mosbrucker et al. (2015) and Haque and Adhikary (2016). Remote sensing literature particularly in freshwater bodies, have shown that there are no unified colour channels that can be used to predict SSC (Pereira et al. 2019). This is due to the multiple parameters that dynamically influence one another as illustrated in Chapter 1.2. That being said, a majority of the literature agrees that the Near-Infrared (NIR) channel is important in estimating SSC. This was demonstrated by a study by Witte et al. (1981) which showed through laboratory experiments that increasing the SSC values increases the reflectance linearly between the red and NIR band. This would suggest that the red channel should have provided the strongest fit.

It is suspected that the choice in the green and blue channel could be due to the ratio of organic and inorganic material found in the collected sediment. In areas with very high coloured dissolved organic matter (CDOM) concentrations such as black water rivers which is most common in peat swamp hydrology, the blue band has been shown to provide strong relations with

SSC (Nichol 1993). Loss of Ignition (LOI) tests using a subset of sample sediment used in the lab experiment indicated that SSC contained 5% organic matter. The small organic percentage in the sediment is too low to suggest that the organic material is a factor for green and blue channel to be favoured. Thus, this factor is ruled out. The reason why the blue and green channel has the strongest fit remains unclear.

3.4.4 Influence of camera type on DN values and implications

A standardised approach for monitoring SSC from close-range remote sensing has so far not yet been converged upon. One of the major challenges to the widespread use of consumer-grade cameras for close-range remote sensing of SSC in rivers is that different camera sensors may influence the relationship between SSC and DN in different ways, and this would make it challenging to compare DN values from different cameras. Some authors have used cameras modified by replacing the standard filters with multispectral sensors to match those of the Landsat 4-5 satellite: Vogt and Vogt (2016) for example replaced the UV/NIR filters of a GoPro HERO3 with an external multiband-pass ZB2 (violet) filter to suppress UV, green, and red wavelengths. This provided blue and NIR sensitivity in the sensor's blue and red channels, but such modification is not likely to be possible in large scale, multi-user citizen science surveys. Unmodified and, ideally, inexpensive cameras are needed for this.

Unmodified cameras have been used in several studies, but different authors have typically developed their own way of treating pixel information to estimate SSC or turbidity. Methods have differed in their complexity, some directly use DN values extracted from images (Bejestan and Nouroozpour 2007; Haque and Adhikary 2016) and others include atmospheric correction, which requires capturing images of the sky and a grey card at the same time as the water surface to account for sky irradiance before assessing correlation with SSC (Leeuw and Boss 2018). Choice of colour band has also varied as stated previously, as has the way values from the many pixels making up a single image are integrated (see Chapter 3.3.3). Mosbrucker et al. (2015) used the maximum pixel value in the blue band and found a good fit for river SSC. However, when the maximum DN values were used in the experiment, the models provided a poor fit as compared to the mean and median DN values. The present study found that across camera sensors and differences in bed colour, the blue and green channel have the strongest fit.

Both cameras used in the lab experiment have the same CMOS sensor but different sensor size. Crisp (2013), states that the size of the sensor determines the dynamic range of the camera where a larger sensor allows more light and vice versa. This is translated into the range of DN

values for each camera. The DJI Mavic Pro drone camera has a sensor size of 1/2.3" while the Vivo V9 (rear) camera does not provide the dimensions for the sensor size. However, smartphone cameras due to their small size have an average sensor size comparable to that of the drone sensor at 1/2.5" (Triggs 2020). The chi-squared test has shown that the DN range between the two cameras was statistically different with the drone camera having a wider range of DN values than the phone camera. This has serious outcomes when selecting a suitable camera for estimating SSC. Small changes in sediment loads in rivers can have marked ecological effects. For example, when DN value is 50, the Brown-Drone-Blue model estimates SSC at 0.05 g/L while the Brown-Phone-Blue model estimates SSC at 0.2 g/L. This phenomenon is consistent across all models. Estimating SSC is especially critical in monitoring sediment sensitive species such as invertebrate assemblages that can drastically drop in species richness and diversity from minute increase in SSC Buendia et al. (2011). Thus, the application of an inappropriate model (a model developed for one camera being used to predict SSC from DN values for an image taken with another camera) may lead to overestimation or underestimation of ecological effects. Additionally, the results indicate that although the phone camera has a narrower DN width, the sensors can predict higher SSC values as compared to the drone camera. E.g. The Grey-Drone-Green model has a maximum predicted SSC of 0.4 g/L while the Grey-Phone-Green has a maximum SSC of 0.6 g/L. It can be argued that the width of the DN is more important as it involves with the accuracy of SSC values than the maximum threshold of SSC. A high SSC threshold does not provide any meaningful prediction if the model is not accurate. Future experiment can focus on field-based calibration and validation between the two camera sensors to examine which cameras sensors are the best at predicting SSC.

3.4.5 Influence of bed colour on DN values

The largest and most obvious influence of bed colour towards the experiment is that the models change in direction when subjected to different bed colour. As to the reason why the change in direction for the Grey tile (negative) and Brown tile (positive), this is due to the relative DN value of the bed colour and fine sediment colour. If the DN of the bed is much lower than the DN of the fine sediment colour, then increasing the concentration of fine sediment would produce a ratio colour that moves towards a higher DN value i.e. a positive relationship. Conversely, if the position of the DN of the bed is much higher than the DN of the fine sediment colour, then increasing the concentration of fine sediment would produce a ratio colour that moves towards a lower DN value i.e. negative relationship. This demonstrates that models produced from a particular river channel

may not be transferable to other rivers due to differences in bed colour. This can even be extended to the colouration of the SSC as the inorganic material of fine sediment are derived from the geology of the catchment. Furthermore, as brought up in Chapter 3.3.2, the presence of a breakpoint is undeniable in the Grey tile while it is much less evident in the Brown tile. This would suggest that the darker Brown tile allows the estimation of higher SSC values than the lighter Grey tile. This could be the reason to why there are no records of a threshold in previous literature as (although not stated) the Brown tile would likely reflect most riverbed colours. However, this only applies on some SSC-DN combinations of the Brown tile. The threshold is evident for the blue channel in this study even though no threshold was observed in the study by Mosbrucker et al. (2015). Replication of this experiment needs to be conducted for a variety of bed colours in order to observe whether the threshold is present. Furthermore, more research could be done on whether the models produced in a river reach could be used to estimate SSC values within the same basin as they would share similar geological conditions. It is also important to note that the effects of bed colour would decrease as the depth of the water increases as discussed in Chapter 1.2.2.

3.5 Conclusion

This chapter aimed to answer three key questions. 1) What are/is the statistically best colour channels to estimate SSC? The models have shown that the green and blue colour channels were statistically the best colour channel across camera sensors with the Grey tile favouring both the green and blue while the Brown tile favouring the blue colour channel. 2) Do different cameras sensors affect the quality of estimation? The quality of estimation of the drone and phone is statistically different through a chi-squared test. The model estimation from the drone camera has a wider DN range than the phone. The differences in DN range results in the overestimation or underestimation of SSC values. The phone model, however, has a higher estimation of SSC than the drone across models. 3) Does the change in bed colour affect the estimation of SSC? The influence of bed colour resulted in the direction of the model completely changes due to the bed colour from a negative (Grey bed) to a positive (Brown bed) relationship. This experiment has led to an unexpected discovery of a maximum threshold in estimating SSC values when using low-cost cameras which have not been recorded in previous papers. The presence of a threshold is less evident in some combinations of the Brown bed while the Grey bed shows clear evidence of a threshold.

4. Chapter 4 Application of aerial surveys to develop suspended sediment maps of river reaches

4.1 Introduction

There is growing interest in remote sensing of rivers to monitor water quality. Water monitoring stations provide relatively sparse information about spatial variation in water quality. Remote sensing has been used to fill this gap for some water quality parameters, including suspended sediments, temperature, and chlorophyll a (which is indicative of nutrient pollution). Despite the increasing popularity of satellite remote sensing for monitoring water quality, particularly in monitoring suspended sediment (e.g. Tomsett and Leyland 2019; Deithier et al. 2020), there are various limitations faced by this technology, as explained in Chapter 1.2. One such limitation mentioned was its spatial resolution. Satellite remote sensing is limited to larger rivers as the typical spatial resolution of freely available satellite imagery is 10-30m, and a minimum of around 2m. Thus, finer-scale variation in sediments or nutrients, which can play an important role in the suitability of habitats for aquatic organisms, cannot be differentiated using satellite remote sensing (Isidro et al. 2018; Yadav et al. 2019; Gallay et al. 2019). In addition, weather conditions can greatly impede data collection particularly cloud cover that directly obstructs the object in focus and reduces data quality through shadows. This is a greater problem in tropical regions where it is extremely hard to obtain <10% cloud cover (Sano et al. 2007) even during dry seasons. These challenges mean that the use of satellite-based remote sensing to monitor small river systems is difficult. The increased availability of low-cost unmanned aerial vehicles (UAVs or drones) has led to an expansion in the use of this technology for a range of environmental monitoring applications (Tomsett and Leyland 2019). Close-range remote sensing using cameras mounted on drones generates images at a higher spatial resolution than satellite-based remote sensing and with less interference from cloud cover (Fig. 1.2), this opens the potential for water quality monitoring in small rivers. This is especially practical in tropical countries such as Malaysia where high-intensity rainfall coupled with extensive land cover change is generating high sediment concentrations in rivers (Chakrapani 2005; Sun et al. 2019). First, to third-order river channels are a major source of sediment inputs in a typical river network (Chappell et al. 2004), meaning that monitoring and detection of high sediment concentrations in small rivers is an important aspect of understanding sedimentation hotspots in tropical water catchments. The value of drones is emphasised by the limited number of conventional monitoring stations. E.g.

there are only eight suspended sediment monitoring stations throughout the three river basins of the most populated state in Malaysia – Selangor (Department of Irrigation and Drainage n.d.).

This chapter builds on the results obtained in the laboratory experiments in Chapter 3. The experiments demonstrated that a good relationship can be derived from Digital Number (DN) to estimate Suspended Sediment Concentration (SSC) through laboratory tests. However, the laboratory experiments also found that relationships are site-specific and camera-specific partly due to the influence of bed colour that can drastically change the direction of the relationship. This chapter explores the application of the approach from Chapter 3 i.e. to estimate SSC in the field using a drone mounted sensor. Chapter 4 begins by using images captured from the same drone camera used in Chapter 3 (DJI Mavic Pro) to quantify spatial variation for a section of the Semenyih River. These relations were then used to produce a map of SSC, which was then validated using spot measurements of sediment concentration. This chapter addresses objective 3 of this thesis: Assess whether it is possible to use DN to reliably predict spatial patterns of SSC across a river reach. The chapter addresses three research questions:

1. Can significant relations between DN and SSC be found using aerial images of a river taken from a drone-mounted camera?
2. Can these relations be used to reliably predict SSC values and produce 'maps' of SSC in a section of the river?
3. What is the magnitude of spatial variation in SSC in a typical section of the river?

4.2 Materials and Methods

4.2.1 Study site

The Semenyih River is one of the main sources of water for over 1 million residents that reside within the basin (Heng et al. 2006) and is essential in supplying water to the agricultural regions which cover the largest percentage of land use type at roughly 40% (Islam et al. 2020). In recent years, the water quality of the Semenyih River has been shown to deteriorate due to increase development and increase in illegal discharge of industrial waste into the river system (Rahman 2014). This has caused frequent and extensive water shortages of clean water over the years and

has prompted the urgency for better monitoring and management of pollution of the Semenyih River (Rahman 2014; Shah 2020).

The study site is a confluence situated adjacent to a recreational area - Sungai Lalang Hotspring (3.04196, 101.87303). The Lalang River is a tributary of the Semenyih River which is part of the larger Langat Basin in Selangor state, Peninsular Malaysia. This study site is located at a river confluence upstream, where the main channel is the Semenyih River while its tributary is the Lalang River. Through observation and satellite images, the tributary experiences higher SSC as its catchment is surrounded by agricultural land use while the main channel experiences lower SSC as it is surrounded by a forested area. This makes the confluence a hydromorphically dynamic area that is likely to contain a wide range of SSC values along a relatively small section of the river. Furthermore, the sediments used in the lab experiment came from the same river which acts as a controlled variable in terms of fine sediment composition in the river.

4.2.2 SSC Measurements

To obtain the SSC values of the study site, 24 metal poles were inserted in the bed of the river to act as sampling points (Fig. 4.1). These poles were inserted in locations that include the upstream of the confluence, tributary, mixing zone of the confluence and downstream channel as well as covering the span of the river– i.e. to capture a range of different SSC values which are representative of this river section. These metal poles were then locally coordinated using a Leica TS60 Total Station with an accuracy of 2mm ± 2ppm. Then, 500 ml of river water was collected from each sampling point. The sampling was conducted on the 22nd January 2020 from 09:30-9:50 am.

SSC values of samples were determined using a vacuum filtration apparatus based on the standard protocol EPA 160.2 (United States Environmental Protection Agency 1999). Firstly, a clean filter membrane was weighed before the filtration process. The filter membrane used for this experiment was Bioflow filter paper: Nylon membrane filter of pore size 0.45 microns. Second, 500ml of water sample was then filtered through the filter membrane and oven-dried at 120 degrees Celsius for 24 hours. Lastly, the oven-dried filter membranes were then weighed and the differences in weight before and after filtration were divided by the volume to derive an SSC in g/L. The 24 samples were later divided into 2 groups; 14 samples were used to derive a calibration relationship, while the remaining 10 was used to validate the calibration model. The 14 SSC values were paired with the DN derived from the orthomosaic to produce an SSC-DN scatterplot.

4.2.3 UAV Imagery Acquisition

Nine Ground Control Points (GCPs) were positioned throughout the left and right bank of the main stem and confluence and were locally coordinated using the Leica TS60 to ensure accurate georeferencing. Once all the water samples were collected, the DJI Mavic Pro drone was immediately deployed to collect images of the channel flown at 30m high. Collecting drone images immediately after sampling is essential to ensure that the images have undergone minimal temporal hydromorphological changes from the time the samples were collected. The drone used in this experiment is the same drone used in the lab experiment in Chapter 3 and act as a controlled variable. The drone camera uses a 14MP CMOS sensor with a sensor size of 6.2 x 4.6mm (1/2.3"). Three flights were needed to capture the full study site with a total flight time of 30 mins (10:00-10:30 am) and a total of 378 images collected. At the time and date of the drone flight, the sun angle was between 35° to 42°. This was done to reduce specular water reflection (sun glint). The weather during the experiment was sunny with sparse cloud cover. The in-built white balance of the drone camera was pre-set to 'sunny' which was adjusted according to the physical white balance card to ensure that DN values can be retrieved from white images and black images. This ensures an optimal dynamic range of the subsequent images. The camera settings were ISO 200, shutter speed 1/600 sec and aperture F2.2.

4.2.4 Calibration, Validation and Production of Orthomosaic

All Red, Green, Blue (RGB) images were processed and stitched using the Pix4dmapper Version 4.6.3 (Pix4D) to produce a continuous orthomosaic. Image analysis was conducted in ArcGIS Version 10.5.0.6491 (Esri). To provide an accurate scale of the study site, the orthomosaic was georeferenced to the local coordinates using the 9 GCPs to increase the absolute accuracy. This was also needed to identify the exact locations of the sampling points on the orthomosaic. At each of the 14 sampling points (calibration points), an area of 100cm² was drawn on the orthomosaic using the 'pixel inspector' tool from ArcGIS. The pixel inspector tool provided the DN values of the R, G and B colour channel that lie within the 100cm². The pixel resolution of the orthomosaic was 1cm² for 1-pixel thus 100cm² occupied exactly 100 pixels and produced 100 DN values of the RGB channel. An average of the DN values for each colour channel was then produced. SSC-DN models were fitted to identify a statistical relationship using the p-value and R² for each colour channel. The strongest model denoted with a high R² was then used to produce an SSC map of the site. In ArcGIS, the selected colour channel is exported as a separated TIF file from the orthomosaic and a polygon shapefile was used to outline the whole river section. The polygon was then used as a template to clip the extent of the orthomosaic using the 'clip raster' tool. The clipped

orthomosaic of the single colour channel was then used to calculate the estimated SSC by applying the equation from the model using the 'raster calculator' tool in ArcGIS.

From the SSC map produced, the validation process requires the comparison of estimated SSC values and the observed values. I used the 10 sampling points as the observed value and compared the estimated value at the locations. The strength of the relationship was then verified by the p-value and R^2 .

4.3 Results

4.3.1 Orthomosaic

Fig. 4.1 shows the orthomosaic of the study site with each sampling points labelled. The area of the orthomosaic covered $0.013 \text{ km}^2/1.2861 \text{ ha}$ with an average ground sampling distance of 1.01cm . 100% of the images were successfully calibrated (378 images out of 378 images calibrated). The GCPs have an accuracy of 1cm in the XY axis and 2cm in the Z-axis with a root mean square error of 10.461 cm (X), 8.936 cm (Y), and 12 cm (Z). The GCPs provide scale and allow accurate measurements of the orthomosaic.

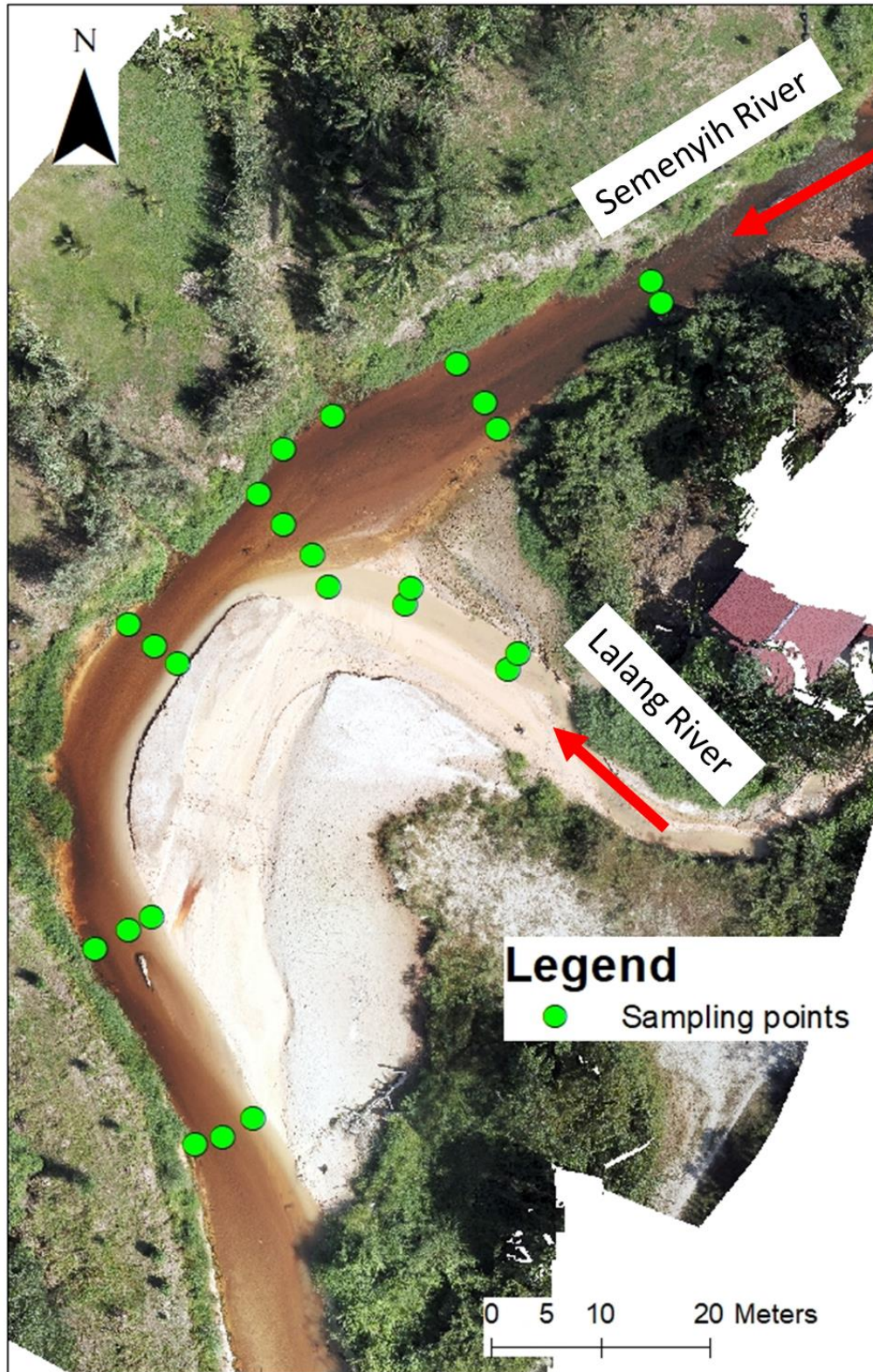


Fig. 4.1 The study site is at a river confluence with the Semenyih River as the main channel and the Lalang River as the tributary. Red arrows indicate flow direction for each river. Green circles indicate the location of water sampling points.

4.3.2 DN v SSC Calibration and Validation

The lowest SSC recorded is 0.0038 g/L while the highest SSC recorded is 0.6524 g/L ($\mu=0.1054$ g/L, $\sigma=0.2099$ g/L). There are two outliers of 0.5264 and 0.6524 g/L which are the two upstream most sampling point of the tributary in Appendix 2. Fig. 4.2 depicts the x-y scatter plot of the SSC vs Red, Green, Blue DN. The scatter points indicate that there is a gradual slope from 0.0021-0.0084 g/L until the slope increases drastically from 0.0084-0.652 g/L which is synonymous with an exponential curve. When fitting a trend line, the exponential function has the strongest R^2 as compared to other function such as the quadratic function at $R^2 > 0.74$ and > 0.5 respectively. The trend line is a positive relationship thereby as SSC increases DN increases. Among the RGB channels, the blue channel has the strongest R^2 followed by the green and red at 0.82, 0.80, and 0.75 respectively. There is a gradual increase in SSC at low DN values but a wide range of SSC at high DN values. The large scatter is akin to the threshold seen from the laboratory tests in Chapter 3. A range of sampling points between 0.1-0.7 g/L would indicate if there is a clear threshold as seen in Chapter 3. The blue colour channel is used to calibrate the orthomosaic of the field site to produce the SSC map as seen in Fig. 4.4.

The model of the observed and predicted SSC values is shown in Fig. 4.3 represented by the dashed line gave an R^2 of 0.8491 and $P < 0.001$. R^2 indicates that roughly 85% of the variation in the observed SSC is explained by the variation in the predicted SSC. When compared to the solid line which represents an accurate prediction of the model ($y = x$), the current model has a slope of 0.69 which underestimates the observed values ($y < x$) – when the predicted value is 0.6 g/L, the observed value is actually 0.04 g/L. Despite the high R^2 , the estimation of SSC through DN decreases in accuracy as the model is systematically over predicting from the solid line.

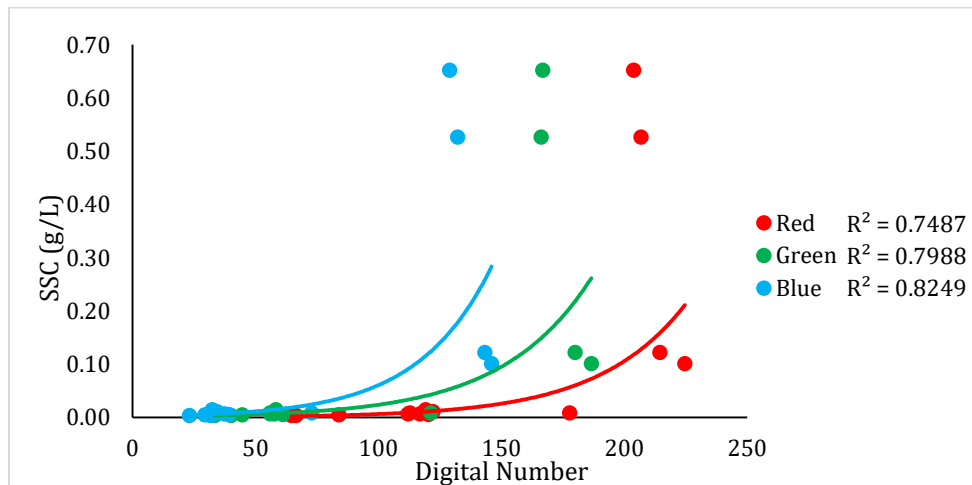


Fig. 4.2 Field calibration of the SSC and DN values for RGB.

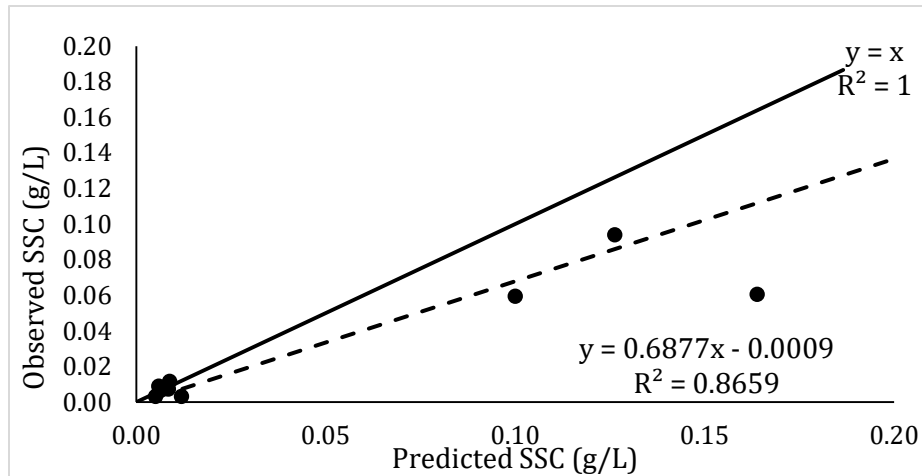


Fig. 4.3 Observed v Predicted SSC values (dashed line) based on the calibration of the blue band. The solid line represents the 1:1 line.

4.3.3 Spatial Distribution of SSC

Fig. 4.4 represents the SSC map of the study site using the calibration model from the blue colour channel. The highest SSC estimated is 7.4498 g/L and is located at the tributary while the lowest SSC estimated is 0.0021 g/L. Most of the study site is estimated to have SSC < 0.5 g/l with the upstream main stem at < 0.025 g/L indicated by the blue hue. The mixing zone between the main stem and tributary is represented by a multi-coloured thin line that straddles the sandbar. The tributary has SSC values >0.5 g/L while the main stem has an SSC value <0.5 g/L, with the main stem having little variation in SSC as compared to the tributary at $\sigma=0.0025$ g/L and $\sigma=0.254$ g/L respectively.

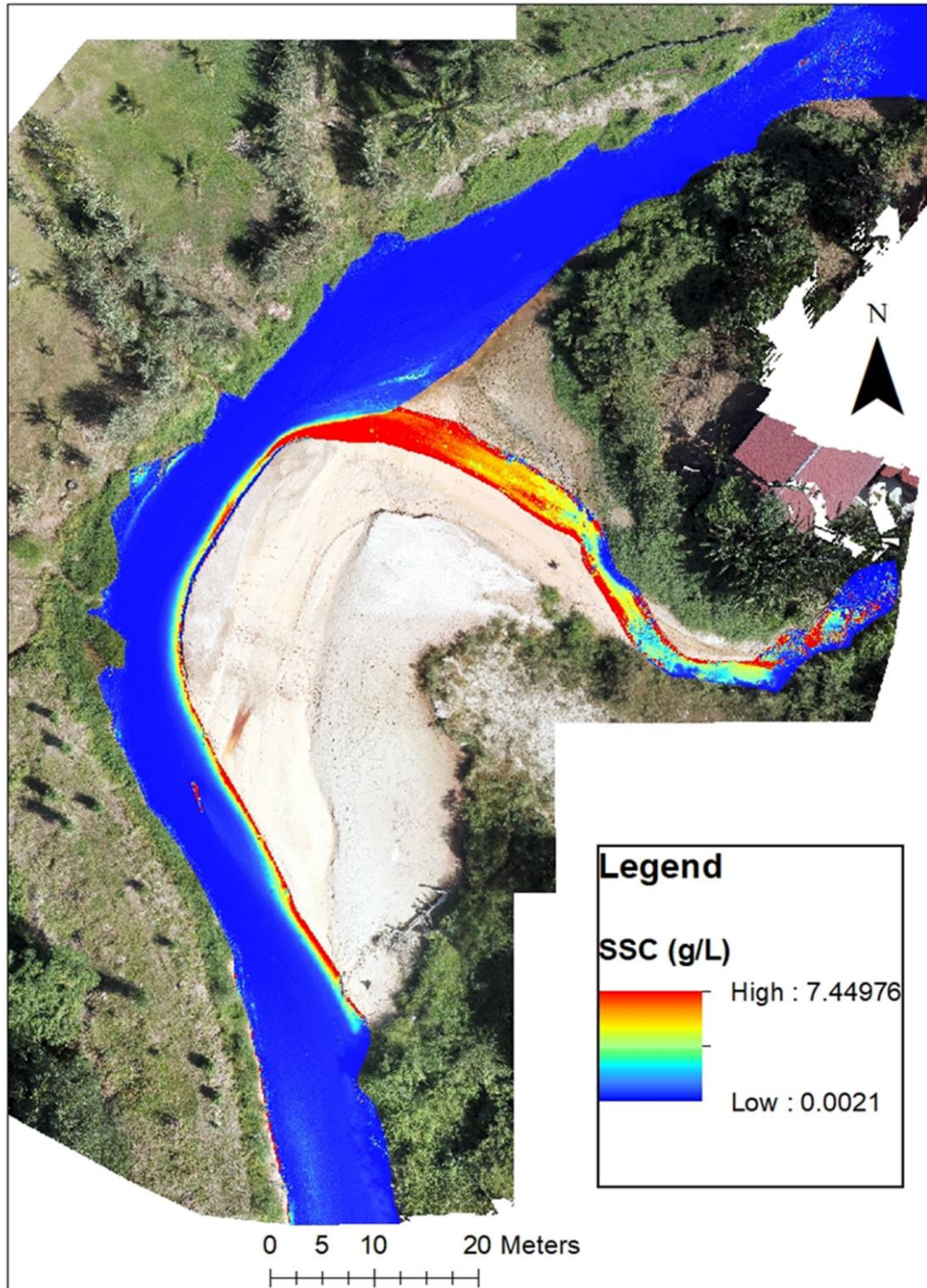


Fig. 4.4 SSC map of the Sungai Lalang Hot spring showing spatial variation in SSC at the confluence of Lalang River and Semenyih River.

4.4 Discussion

4.4.1 Spatial Distribution of SSC

The SSC map from Fig. 4.4 has provided valuable insight into the hydromorphic conditions of the river confluence. The Semenyih River has a significantly lower SSC value than the Lalang River which is reflected from predicted SSC values from the SSC map. The low SSC values from the main stem could be attributed to the Semenyih dam situated 3 km upstream which would inhibit natural sediment transport. The highest predicted SSC value is 7 g/L which is from Sungai Lalang despite observed SSC values from this area only reaching up to 0.6 g/L. The over prediction of SSC is a result of the systematic over prediction of the calibrated model (Fig. 4.3) which only decreases in accuracy as the observed SSC values increases. This over prediction is due to the limited sample size of only 24 sample points taken in the field where 14 sample points were used in the calibration stage and the remainder used for validation. The limited sample size was not able to acquire a wide set of SSC values that can produce a model that reflect the nature of the confluence.

In addition to the over prediction of SSC due to the model, high estimates of SSC values in some areas of the river may also be due to the estimation of the riverbed DN instead of the water column due to the shallow depth of Sungai Lalang (average 0.16 m depth v 0.38 m in Sungai Semenyih). This effect can be confirmed by observing the left bank of the downstream channel, the red areas across the left bank are capturing DN values of the sandbar hence why it is perceived to have a higher SSC. Areas of the upstream tributary display low SSC (seen in blue) intermix with high SSC (seen in red). Whereas the high SSC value is a result of the camera capturing the riverbed instead of the water column. SSC analysis must be taken into consideration of false estimation of SSC by the influence of riverbed, as was demonstrated by the laboratory experiments in Chapter 3, and highlights the importance of accounting for water depth and bed topography before using drone-based cameras to quantify SSC in small streams and rivers

Fig. 4.4 shows that despite the high SSC in the tributary there is no evidence of a spatially extensive mixing zone; instead of forcing its way out into the main channel, a narrow channel of higher SSC is evident along the left bank adjacent to the sand bar. This pattern may however be discharge specific, as a function of the relative discharge magnitude in the tributary and main stem. In the low flow conditions prevailing during the current flights, velocity in the tributary was low compared to the main stem (0.15 and 0.5 m/s respectively) and so lacked the momentum to create an extensive mixing area. However, under different prevailing conditions, the pattern of mixing and hence SSC may be very different.

4.4.2 Mapping SSC Distribution in small rivers

Although the strongest model relationship of SSC-DN is the exponential function, the strength of the relationship between SSC and DN deteriorates as the SSC increases. Fig. 4.2 shows that the exponential trend line cannot fit observed SSC >0.3 g/L indicating that SSC estimations are more reliable at lower values. The reasoning for the choice of selecting a simpler function as opposed to GAMs was based on the smooth trend line of the GAMs in the lab experiment where a simpler function would suffice for the field test. The choice of the blue colour channel is consistent with the calibrations from Chapter 3 which also favoured the blue and green colour channel. This matches previous studies of close-range remote sensing for measuring SSC concentrations by Mosbrucker et al. (2015) and Haque and Adhikary (2016). However, other studies have found different optimal colour bands and statistical relationships for estimating suspended sediment (Dang et al. 2018; Isidro et al. 2018; Pereira et al. 2019; Gallay et al. 2019). This is due to the complex interaction between different parameters (e.g. fine sediment and benthic composition, river depth, and bed topography) affecting the visual characteristics of aquatic environments (as discussed in Chapter 1.2) that may prevent a unified model for remote sensing of water quality characteristics. These parameters are partly explored in the following sections.

According to on-site field observation, despite the difference in bed colour between the tributary which has a lighter bed colour than the main channel, the overall trend line of the model is a positive relationship i.e. as DN increases, SSC increases. In retrospect from the lab experiment from Chapter 3, the lighter grey bed colour has a negative relationship whereas the darker brown bed colour has a positive relationship. The change of direction between both bed colours was due to the contrast between the DN value of each bed colour against the suspended sediment colour. The field tests inform us that despite the contrasting bed colours in the field, both bed colours have a lower DN value than the fine sediment colour. Another prevailing influence is river depth concerning bed colour. In principle, river depth is inversely related to bed colour, i.e. the shallower the river, the greater the influence of the bed colour in the estimation of SSC and vice versa. In this instance, the shallow depth of the tributary has resulted in the overestimation of SSC to an unreasonable value of 7 g/L (seen in red) despite the observed samples measure to only 0.6 g/L. Estimation of SSC at shallow river depths has proven to be unreliable due to the overarching influence of the bed colour.

Additionally, the accuracy of predicting SSC is affected by riparian shade, the shadows cast onto the water surface blocks direct sunlight which prevents accurate reading of river DN (Shahtahmassebi et al. 2013). This effect is observed in Fig. 4.5 in the upstream region of the tributary where it is estimated to have lower SSC (seen in blue) than the rest of the tributary (seen

in orange and red). Due to the small width of the tributary, the influence of riparian shade greatly exacerbates the ability to obtain usable information. This relates to the parameter of River Width under the factor ‘River Physiography’ from the conceptual diagram discussed in Chapter 1.2. De-shadowing algorithms can be applied to remove or relax the impacts of shadows (Shahtahmassebi et al. 2013). One such algorithm was used by Shahtahmassebi et al. (2011), to reduce the effects of topographic shadow by restoring information in shadow areas based on surrounding information. This was proven simple and cost-effective but require a homogenous landscape to ensure accurate removal of shadows. Filippi and Güneralp (2013) developed a de-shadowing algorithm specifically to cater for riparian vegetation and have proven to significantly increase classification accuracy and improves detection. This method however requires the use of hyperspectral images which is not possible for low-cost drones. More research can be done to explore the effectiveness of de-shadowing algorithms in narrow rivers using RGB sensors.



Fig. 4.5 Effects of riparian vegetation on the estimation of SSC. The left image shows the orthomosaic section of the upstream tributary which is greatly covered by vegetation while the right image is the SSC map derived from the orthomosaic.

4.4.3 Use of fine-scale SSC maps for ecology and conservation

Despite the potential sources of inaccuracy described above, the very high spatial resolution (1cm^2 /pixel) of the SSC map can quantify small-scale differences in SSC within a section of the river. High spatial resolution SSC maps can be an important tool for monitoring small-scale spatial changes in SSC to understand the relationships between species and habitat (Owens et al. 2005; Marteau et al. 2020a, b). Despite considerable research, there is little agreement on the ecological effects of suspended sediment as a function of concentration and duration of exposure (Newcombe and Macdonald 2011; Jones et al. 2012). This research can be used to study the response of targeted species in hydromorphically dynamic areas such as river confluences or regions that experience intensive LULCC. The range of suitable and unsuitable SSC conditions for aquatic species can be used to partition the SSC values accordingly in the map which will then be turned into a map of habitat suitability for the targeted species. Marteau et al. (2017b) conducted

a study on the effects of fine sediment dynamics from the reconnection of the Ben Gill tributary towards the Ehen River. Their studies show that the reconnection of the tributary resulted in a 65% increase in sediment load into the river system. The current method can be used to regularly monitor temporal and spatial differences of SSC within the confluence particularly for the interest of protecting sediment sensitive species.

In addition to monitoring river ecology. This method can potentially be applied as a proxy to monitor water quality for human consumption. Identifying sources of sediment pollution can be expensive and time-consuming, requiring multiple site inspections and sample processing at each point source in different LULCCs. Drone-based remote sensing can be applied to survey multiple sites to identify fine sediment hotspots before deploying in-situ site sampling and analysis. Although water management bodies measure suspended sediment in turbidity and Total Suspended Sediment (TSS), cross-calibration on a site by site basis can be applied to derive turbidity and TSS values from SSC in order to match the Water Quality Index classes for Malaysian water monitoring (Glysson et al. 2000; Pavanelli and Palgiarani 2002).

Although this study has shown the potential effectiveness of the models, the study has also highlighted key constraints that can be further explored and built upon before being utilised by the public. These constraints are 1) the model is over predicting observed values as SSC increases which is evident in Fig. 4.3, and 2) these models cannot accommodate variations in bed colour that are different to the study site according to the lab experiments conducted in Chapter 3. Hence the models are site specific; this means that new models should be developed for each site. This is discussed further in Chapter 5.

4.5 Conclusion

This chapter aimed to answer three research questions. (1) Can significant relations between DN and SSC be found using aerial images of a river taken from a drone-mounted camera? Strong statistical relations were found using consumer-grade drones with an RGB sensor to monitor suspended sediment in river systems. (2) Can these relations be used to reliably predict SSC values and produce 'maps' of SSC in a river section? Our results have demonstrated that through in-situ sampling, the estimation of SSC is proven to have strong predictive power ($R^2 > 0.8$), however the model over predicts SSC values. Due to the high spatial resolution and accuracy of the estimation, this method provides great promise towards understanding the effects of small-scale fluvial dynamics within ecosystems. Results of the present study however suggest that the influence of riverbanks, riparian shading and water depth are primary sources of inaccuracy as discussed in Chapter 1.2. Particularly the effects of shallow river depth greatly amplify the ratio of riverbed

colour concerning fine sediment colour. Therefore, this technique is likely to be more suitable for monitoring SSC in relatively deep and/or turbid streams and rivers compared to shallow and/or clear water streams where the bed is visible. (3) What is the magnitude of spatial variation in SSC in a typical section of the river? Overall, the SSC map has a fine spatial scale of $1\text{cm}^2/\text{pixel}$. The tributary has an order of magnitude higher SSC ($>0.5\text{ g/L}$) than the upstream main stem ($<0.025\text{ g/L}$), with the main stem having little variation in SSC as compared to the tributary at $\sigma=0.0025\text{ g/L}$ and $\sigma=0.254\text{ g/L}$ respectively. This method shows great potential offering a cost-effective approach to SSC monitoring in narrow streams and rivers in the tropics.

5. Chapter 5. Conclusions

5.1 Synthesis

The studies conducted in Chapter 3 and Chapter 4 have shown that the mathematical relationship between estimated SSC (from DN in camera images) and measured SSC in laboratory conditions cannot be directly applied to estimate SSC in the field. This is due to the interaction of bed colour and relative colour of suspended sediment. Different relations of different sites mean that the best approach is to develop specific calibration for each location.

The laboratory experiment has also provided clear evidence that the types of cameras used will affect the quality of estimation driven by the camera sensor size which determines the range of DN received by the sensor. Larger camera sensors are more favoured as they can capture a wider range of DN values which will increase the accuracy of SSC estimation. The phone sensor due to the smaller sensor size provided a narrower DN range as opposed to the drone camera that has a larger sensor size hence wider DN range. This may only act as a temporary limitation for phone cameras as newer phones are adopting larger camera sensors as consumer demand for better image quality rises (Diamandis and Kotler 2020).

Additionally, an SSC threshold was detected throughout the study (Chapter 3), where further changes in SSC concentration could not be distinguished by DN values providing no meaningful SSC estimation. This observation has not been recorded in previous studies. The SSC threshold was evident in the laboratory where the trend line linking SSC and DN deteriorates above an SSC concentration of 0.2 g/L- 1 g/L and was observed across all tile colour, camera and colour channel combinations with the exception of the Brown tile where the threshold was not as clear. The inclusion of values above the threshold would severely impact the models produced due to the high scatter within the y axis. The diminished presence of an apparent breakdown for the Brown tile seems to indicate that the darker bed colour can still produce meaningful DN values as SSC increases. This would also suggest that the breakdown was not a result of an experimental artefact. This study suggests that the cause could come from limited sensor capabilities of the cameras or that the breakdown is dependent on the apparent colour of the bed in relation to the colour of fine sediment within the water column.

Estimation of SSC in the field requires field calibrations that ideally should include samples with a wide range of SSC values. Despite the potential of this methodology to generate valuable new information about spatial variation in SSC, particularly in the tropics where fine sediment monitoring networks are typically sparse, there are several key limitations which must

be considered before this approach can be widely applied: 1) The effects of shallow river depth which amplify the influence of bed colour relative to fine sediment colour, and 2) the difficulty of estimating SSC in small tributaries due to riparian shading which covers a larger proportion of the river surface compared to larger rivers.

The findings of the present study indicate that 1) estimating SSC through DN is possible and does not require the conversion of DN value to reflectance value while still providing a strong model fit, 2) larger camera sensors are required to provide an accurate estimation of SSC and that camera sensors from smartphones are currently inadequate, 3) calibrations are site-specific and require in-situ sampling for each new site, and 4) SSC concentrations above a threshold value are difficult to measure using digital images. This last finding may be particularly important for the potential use of digital cameras to monitor SSC in tropical rivers, where SSC values are typically higher than in temperate streams and rivers

5.2 Limitations

In hindsight, there were many limitations faced and have been made clear throughout the process of completing this study. The lack of available literature on estimating SSC through DN values was a core limitation. Although many studies employ reflectance values, there was a large gap in exploring the utility of low-cost cameras to estimate SSC using DN about which only three papers exist: Bejestan and Nouroozpour (2007), Mosbrucker et al. (2015), and Haque and Adhikary (2016). Due to the limited literature on the subject matter, multiple knowledge gaps were needed to fill, particularly the applicability of smartphone and drone cameras, the influence of riverbed colour on the estimation of SSC and model functions derived from these parameter combinations.

Another clear limitation is the limited sample size from the field tests, obtaining sample sizes larger than the current study could produce a better prediction as the data collected have shown that there is a gap of SSC values measured in the field between 0.1 g/L and 0.7 g/L seen in Fig. 4.2. The gap in SSC values within the 0.1-0.7 g/L range was simply due to only having five sampling points within the tributary. A larger sample size that captured SSC values within this range could identify the possible presence of a threshold as seen from the laboratory experiment.

5.3 Future Research

Several knowledge gaps remain concerning the use of remote sensing tools and digital images to estimate SSC in rivers. The conceptual diagram (Figure 1.2) is mostly populated with studies that focuses on reflectance values and not DN values. One of the most important areas for future

research would be direct comparisons between models estimating SSC from DN and those using reflectance values. Another useful research avenue would be to compare the model fits of different smartphone cameras. This study compared a Vivo V9 smartphone camera with a DJI Mavic Pro drone camera which has shown that the smaller sensor size of the phone camera as compared that to the drone camera makes it less accurate at predicting SSC. Smartphone camera technology is improving rapidly, and already there are many new models that may produce better predictions than reported here. Thus, a study comparing across multiple high spec mobile phone cameras may prove insightful. Another important gap concerns the influence of different bed characteristics on estimates SSC. This thesis and other recent studies have shown the influence of bed colour, but no one has yet looked for example at how shadows produced by gravel beds could influence DN values, and in turn how this might affect estimates of SSC.

On a larger scale, future research can be done on the applicability of low-cost drones in estimating SSC at a catchment scale. Having a SSC distribution map is useful for ecological studies. For example, invertebrates are known to be sensitive to increase in SSC because it can increase gill damage (Beussink 2007). Researchers can use these maps to structure a sampling program within a stream reach and sample invertebrate populations from places that have consistently higher and consistently lower SSC to observe levels of gill damage. Patterns of spatial variation in SSC across a stream reach may vary over time (e.g. as a function of discharge) so SSC maps could also be used to look at how rapidly (or otherwise) invertebrate distributions change in response to spatial patterns of high and low SSC across a reach. Increases in SSC have also been found to initiate an increase in invertebrate drift (Behar et al. (2019)). SSC maps would be used to explore this at fine spatial scales, to assess differential patterns of drift loss across a reach as a result of variation in SSC. The method could be applied to help with management. For example, the impacts of oil palm plantations on SSC have not been extensively studied. This new method can very easily survey along the main stretch of a river to quantify the contribution and mixing of SSC from oil palm plantations, to identify contamination sources and, accordingly, target mitigation (better land husbandry, better riparian management etc.). The fact that cameras can be used to assess suspended sediment also opens the possibility for them to collect temporal data; for instance, time lapse cameras could be used to take images at specified time interval, much the same way that turbidity sensors log NTU values. Thus, they may have utility as an alternative to turbidity sensors. All such studies would be valuable to help understand spatio-temporal variation in SSC and how this affects aquatic communities.

Another application of camera sensors is water quality monitoring through citizen science. Citizen science is defined as the active public involvement in scientific research (Irwin

2018). Individual citizens could, in theory, simply take an image of a river that they have an interest in and this could be used to compute SSC using a mobile application. This opens up the possibility for co-ordinated, geographically extensive citizen surveys of SSC. For this to be possible, research is needed to assess transferability of SSC models across smartphone devices of different camera sensor quality. Technology companies are increasingly successful in converging smartphone technology with photographic hardware. Sensors and lenses have improved with successive smartphone models and are now comparable to that of compact cameras in some aspects, but work is still needed to assess the consistency (or otherwise) of DN-SSC models. If they differ, the prospects for citizen science would be undermined by having to have models for each phone model.

5.4 Concluding remarks

This study provides insight into the applicability of using low-cost cameras to estimate SSC using DN values. Additionally, this study also examined the influence of different bed colours and different camera sensors towards the estimation of SSC using DN. In chapter 3, it can be concluded that uncalibrated DN values can be used to estimate SSC. The estimation of SSC can be conducted using different camera sensors but the model estimates are not transferable between different camera sensors (smartphone, drone). The influence of different bed colours substantially changes the direction of the model estimates and hence indicates that model estimates are not transferrable across rivers. In chapter 4, it can be concluded that it is possible to use DN to reliably predict spatial SSC across a river reach with great accuracy ($R^2 > 0.8$) and produce high resolution SSC distribution maps ($1\text{cm}^2/\text{pixel}$). The accuracy of model estimates is further improved if the river bed is not visible (ensuring no river bed reflectance) and there is an absence/minimal shadows on the river surface. These findings provide important insights into the potential application of this methodology for freshwater ecological research and water quality monitoring and management. However, more research is required before this technology can be utilised for citizen science water quality monitoring programmes.

References

- Abd Manap M, Nampak H, Pradhan B et al (2014) Application of probabilistic-based frequency ratio model in groundwater potential mapping using remote sensing data and GIS. *Arabian Journal of Geosciences* 7(2):711-724
- Aiello A, Canora F, Pasquariello G, Spilotro G (2013) Shoreline variations and coastal dynamics: A space–time data analysis of the Jonian littoral, Italy. *Estuarine, Coastal and Shelf Science* 129:124-135
- Alashloo MM, Lim HS, Asadpour R, Safarpour S (2013) Total suspended sediments mapping by using ALOS imagery over the coastal waters of Langkawi Island, Malaysia. *Journal of the Indian Society of Remote Sensing* 41(3):663-673
- Amirabadizadeh M, Huang YF, Lee TS (2015) Recent trends in temperature and precipitation in the Langat River basin, Malaysia. *Advances in Meteorology* 2015
- Anees MT, Abdullah K, Nawawi MNM, Norulaini NAN, Syakir MI, Omar AKM (2018) Soil erosion analysis by RUSLE and sediment yield models using remote sensing and GIS in Kelantan state, Peninsular Malaysia. *Soil Research* 56(4): 356-372
- Asadpour R, San LH, Alashloo MM, Moussavi SY (2012) A statistical model for mapping spatial distribution of total suspended solid from THEOS satellite imagery over Penang Island, Malaysia. *Journal of Applied Sciences Research* 8(1): 271-276
- Ayub KR, Hin LS, Abd Aziz H (2009) SWAT application for hydrologic and water quality modeling for suspended sediments: a case study of Sungai Langat's catchment in Selangor.
- Azhari AW, Sopian K, Zaharim A, Al Ghouli M (2008) A new approach for predicting solar radiation in tropical environment using satellite images-case study of Malaysia. *WSEAS Transactions on Environment and Development* 4(4):373-378
- Bartolucci LA, Robinson BF, Silva LF (1977) Field measurements of the spectral response of natural waters. *Photogrammetric Engineering and Remote Sensing* 43(5):595-598
- Basheer AO, Hanafiah MM, Abdulhasan MJ (2017) A study on water quality from Langat River, Selangor. *Acta Scientifica Malaysia (ASM)* 1(2):1-4
- Béjar M, Gibbins CN, Vericat D, Batalla RJ (2017) Effects of suspended sediment transport on invertebrate drift. *River Research and Applications* 33(10):1655-1666
- Bejestan MS, Nouroozpour S (2007) Use of image processing technique to estimate sediment concentration. *Journal of Applied Sciences* 7(20):3096-3100
- Berga L, Buil JM, Bofill E et al (eds) (2006) *Dams and Reservoirs, Societies and Environment in the 21st Century, Two Volume Set: Proceedings of the International Symposium on Dams in the Societies of the 21st Century, 22nd International Congress on Large Dams (ICOLD), Barcelona, Spain, 18 June 2006.* CRC Press

- Beussink ZS (2007) The effects of suspended sediment on the attachment and metamorphosis success of freshwater mussel parasitic life stages (Doctoral dissertation, Missouri State University).
- Bivand R, Keitt T, Rowlingson B (2020) rgdal: Bindings for the 'Geospatial' Data Abstraction Library. R package version 1.5-16. <https://CRAN.R-project.org/package=rgdal>
- Buendia C, Gibbins CN, Vericat D, Batalla RJ (2014) Effects of flow and fine sediment dynamics on the turnover of stream invertebrate assemblages. *Ecohydrology* 7(4):1105-1123
- Buendia C, Gibbins CN, Vericat D, Lopez-Tarazon JA, Batalla RJ (2011) Influence of naturally high fine sediment loads on aquatic insect larvae in a montane river. *Scottish Geographical Journal* 127(4):315-334
- Caldwell RL, Edmonds DA (2014) The effects of sediment properties on deltaic processes and morphologies: A numerical modeling study. *Journal of Geophysical Research: Earth Surface* 119(5):961-982
- Caltest analytical Laboratory (n.d.) Total Suspended Solids Analysis (TSS) and Suspended Sediment Concentration Analysis (SSC). [https://caltestlabs.com/analytical-services/priority-pollutants/inorganic-methods/tssandssc/#:~:text=Total%20Suspended%20Solids%20\(TSS\)%20and,set%20up%20of%20the%20analysis](https://caltestlabs.com/analytical-services/priority-pollutants/inorganic-methods/tssandssc/#:~:text=Total%20Suspended%20Solids%20(TSS)%20and,set%20up%20of%20the%20analysis). Accessed 20 January 2020
- Chakrapani GJ (2005) Factors controlling variations in river sediment loads. *Current Science* 8(4):569-575
- Chappell NA, Douglas I, Hanapi JM, Tych W (2004) Sources of suspended sediment within a tropical catchment recovering from selective logging. *Hydrological Processes* 18(4):685-701
- Crisp S (2013) Camera sensor size: Why does it matter and exactly how big are they. *Luetlavissa*. <http://www.gizmag.com/camera-sensor-size-guide/26684/>. Accessed 26 December 2020
- Dang TD, Cochrane TA, Arias ME (2018) Quantifying suspended sediment dynamics in mega deltas using remote sensing data: a case study of the Mekong floodplains. *International Journal of Applied Earth Observation and Geoinformation* 68:105-115
- Davies-Colley RJ, Hickey CW, Quinn JM, Ryan PA (1992) Effects of clay discharges on streams. *Hydrobiologia* 248(3):215-234
- Dean C, Warner TA, McGraw JB (2000) Suitability of the DCS460c colour digital camera for quantitative remote sensing analysis of vegetation. *ISPRS Journal of Photogrammetry and Remote Sensing* 55(2):105-118
- Dearing JA, Jones RT (2003) Coupling temporal and spatial dimensions of global sediment flux through lake and marine sediment records. *Global and Planetary Change* 39(1-2):147-168

- Dethier EN, Renshaw CE, Magilligan FJ (2020) Toward Improved Accuracy of Remote Sensing Approaches for Quantifying Suspended Sediment: Implications for Suspended-Sediment Monitoring. *Journal of Geophysical Research: Earth Surface* 125(7):1-21
- Department of Irrigation and Drainage (n.d) Selangor-suspended sediment stations. <http://h2o.water.gov.my/v2/fail/Invstations/SDSel.html>. Accessed 26 December 2020
- Diamandis PH, Kotler S (2020) The Future is Faster Than You Think: How Converging Technologies are Transforming Business, Industries, and Our Lives. Simon & Schuster
- Doeg TJ, Koehn JD (1994) Effects of draining and desilting a small weir on downstream fish and macroinvertebrates. *Regulated Rivers: Research & Management* 9(4):263-277
- Dudgeon D, Arthington AH, Gessner MO et al (2006) Freshwater biodiversity: importance, threats, status and conservation challenges. *Biological Reviews* 81(2):163-182
- Durum WH, Heidel SG, Tison LJ (1960) World-wide runoff of dissolved solids. *International Association for Hydrological Science* 51:618-628
- Ekhuemelo DO, Amonum JI, Usman IA (2016) Importance of forest and trees in sustaining water supply and rainfall. *Nigeria Journal of Education, Health and Technology Research* 8:273-280
- El-Alfy MA, Hasballah AF, Abd El-Hamid HT, El-Zeiny AM (2019) Toxicity assessment of heavy metals and organochlorine pesticides in freshwater and marine environment
- Fellgett P (1953) Concerning photographic grain, signal-to-noise ratio, and information. *Josa* 43(4):271-282
- Filippi AM, Güneralp İ (2013) Influence of shadow removal on image classification in riverine environments. *Optics Letters* 38(10):1676-1678
- France MM (1993) Reflections on rippling water. *The American Mathematical Monthly* 100(8):743-748
- Gallay M, Martinez JM, Mora A et al (2019) Assessing Orinoco river sediment discharge trend using MODIS satellite images. *Journal of South American Earth Sciences* 91:320-331
- Geyman EC, Maloof AC (2019) A simple method for extracting water depth from multispectral satellite imagery in regions of variable bottom type. *Earth and Space Science* 6(3):527-537
- Glysson GD, Gray JR, Conge LM (2000) Adjustment of total suspended solids data for use in sediment studies. In *Building partnerships* 104:1-10
- Gobbett DJ, Hutchison CS, Burton CK, Geological Society of Malaysia (1973) *Geology of the Malay Peninsula; (West Malaysia and Singapore)*. New York: Wiley-Interscience
- Goddijn LM, White M (2006) Using a digital camera for water quality measurements in Galway Bay. *Estuarine, Coastal and Shelf Science* 66(3-4):429-436
- Graham AA (1990) Siltation of stone-surface periphyton in rivers by clay-sized particles from low concentrations in suspension. *Hydrobiologia* 199(2):107-115

- Han L, Rundquist DC, Liu LL, Fraser RN, Schalles JF (1994) The spectral responses of algal chlorophyll in water with varying levels of suspended sediment. *International Journal of Remote Sensing* 15(18):3707-3718
- Haque A, Adhikary KK (2016) Estimation of suspended sediment concentration of water bodies using low cost portable digital camera. *Proceedings of 3rd International Conference on Advances in Civil Engineering, CUET, Chittagong, Bangladesh*
- Heng LY, Abdullah MP, Yi CS, Mokhtar M, Ahmad R (2006) Development of possible indicators for sewage pollution for the assessment of Langat River ecosystem health. *Malaysian Journal of Analytical Sciences* 10(1):15-26
- Hoguane AM, Green CL, Bowers DG, Nordez S (2012) A note on using a digital camera to measure suspended sediment load in Maputo Bay, Mozambique. *Remote Sensing Letters* 3(3) :259-266
- Holeman JN (1968) The sediment yield of major rivers of the world. *Water Resources Research* 4(4):737-747
- Hu B, Yang Z, Wang H et al (2009) Sedimentation in the Three Gorges Dam and the future trend of Changjiang (Yangtze River) sediment flux to the sea. *Hydrology and Earth System Sciences* 13(11):2253
- Huang YF, Ang SY, Lee KM, Lee TS (2015) Quality of water resources in Malaysia. *Research and Practices in Water Quality* 3:65-94
- Idrus S, Samad AH (2006) Urban land use change and the Langat basin ecosystem health. *Planning Malaysia* 2(1):51-68
- Isidro CM, McIntyre N, Lechner AM, Callow I (2018) Quantifying suspended solids in small rivers using satellite data. *Science of The Total Environment* 634:1554-1562
- Islam MR, Jaafar WZW, Hin LS, Osman N, Karim MR (2020) Development of an erosion model for Langat River Basin, Malaysia, adapting GIS and RS in RUSLE. *Applied Water Science* 10(7):1-11
- Julien P, Shah S (2005) *Sedimentation Initiatives in Developing Countries Draft Report presented to UNESCO-ISI. Colorado State University.*
- Jones JI, Murphy JF, Collins AL, Sear DA, Naden PS, Armitage PD (2012) The impact of fine sediment on macro-invertebrates. *River Research and Applications* 28(8):1055-1071
- Kass RE, Raftery AE (1995) Bayes factors. *Journal of the American Statistical Association* 90(430):773-795
- Kemp P, Sear D, Collins A, Naden P, Jones I (2011) The impacts of fine sediment on riverine fish. *Hydrological Processes* 25(11):1800-1821

- Khalid K, Ali MF, Abd Rahman NF, Mispan MR, Haron SH, Abd Rasid MZ., ... Kamaruddin H (2016) Application of the SWAT hydrologic model in Malaysia: recent research. The challenges of agro-environmental research in Monsoon Asia:237-246
- Kirk JT (1994) Light and photosynthesis in aquatic ecosystems. Cambridge university press.
- Kobayashi H, Toratani M, Matsumura S et al (2011) Optical properties of inorganic suspended solids and their influence on ocean colour remote sensing in highly turbid coastal waters. International Journal of Remote Sensing 32(23):8393-8420
- Kokhanovsky A (2004) Optical properties of terrestrial clouds. Earth-Science Reviews 64(3-4):189-241
- Kondolf GM, Gao Y, Annandale GW et al (2014) Sustainable sediment management in reservoirs and regulated rivers: Experiences from five continents. Earth's Future 2(5):256-280
- Lal R (1985) Soil erosion and sediment transport research in tropical Africa. Hydrological Sciences Journal 30(2):239-256
- Lee CP (2001) Scarcity of fossils in the Kenny Hill formation and its implications. Gondwana Research 4(4):675-677
- Leeuw T, Boss E (2018) The HydroColor app: Above water measurements of remote sensing reflectance and turbidity using a smartphone camera. Sensors 18(1):256
- Legleiter CJ, Kinzel PJ, Overstreet BT (2011) Evaluating the potential for remote bathymetric mapping of a turbid, sand-bed river: 1. Field spectroscopy and radiative transfer modeling. Water Resources Research 47(9):1-19
- Legleiter CJ, Roberts DA, Marcus WA, Fonstad MA (2004) Passive optical remote sensing of river channel morphology and in-stream habitat: Physical basis and feasibility. Remote Sensing of Environment 93(4):493-510
- Lemon J (2006) Plotrix: a package in the red light district of R. R-News 6(4):8-12
- Leslie AG, Dobbs MR, Tham Fatt N et al (2020) The Ukay Perdana Shear Zone in Kuala Lumpur: a crustal-scale marker of early Jurassic orogenic deformation in Peninsular Malaysia. Bulletin of the Geological Society of Malaysia 69:135-147
- Li Z, Shen H, Cheng Q, Li W, Zhang L (2019) Thick cloud removal in high-resolution satellite images using stepwise radiometric adjustment and residual correction Remote Sensing 11(16):1925
- Liedtke J, Roberts A, Luternauer J (1995) Practical remote sensing of suspended sediment concentration. Photogrammetric engineering and remote sensing 61(2):167-175
- Lim HS, MatJafri MZ, Abdullah K, Saleh NM (2008) Using satellite remote sensing to monitor the total suspended solids (TSS) over Penang Island, Malaysia. International Society for Optics and Photonics 7105:71050Z

- Lyzenga DR (1978) Passive remote sensing techniques for mapping water depth and bottom features. *Applied Optics* 17(3):379-383
- Mantovani JE, Cabral AP (1992) Tank depth determination for water radiometric measurements. *International Journal of Remote Sensing* 13(14):2727-2733
- Marteau B, Vericat D, Gibbins C, Batalla RJ, Green DR (2017a) Application of Structure-from-Motion photogrammetry to river restoration. *Earth Surface Processes and Landforms* 42(3):503-515
- Marteau B, Batalla RJ, Vericat D, Gibbins C (2017b) The importance of a small ephemeral tributary for fine sediment dynamics in a main-stem river. *River Research and Applications* 33(10):1564-1574
- Marteau B, Gibbins C, Vericat D, Batalla RJ (2020a) Geomorphological response to system-scale river rehabilitation I: Sediment supply from a reconnected tributary. *River Research and Applications* 36(8):1488-1503
- Marteau B, Gibbins C, Vericat D, Batalla RJ (2020b) Geomorphological response to system-scale river rehabilitation II: Main-stem channel adjustments following reconnection of an ephemeral tributary. *River Research and Applications* 36(8):1472-1487
- Memarian H, Balasundram SK, Talib JB, Sood AM, Abbaspour KC (2012) Trend analysis of water discharge and sediment load during the past three decades of development in the Langat basin, Malaysia. *Hydrological Sciences Journal* 57(6):1207-1222
- Mertes LA, Smith MO, Adams JB (1993) Estimating suspended sediment concentrations in surface waters of the Amazon River wetlands from Landsat images. *Remote Sensing of Environment*, 43(3):281-301
- Mohd WMNW, Noor AMM, Othman AN (2007) Utilizing satellite-based remote sensing data for water quality assessment of inland water bodies. *Built Environmental Journal* 4:42-51
- Mosbrucker AR, Spicer KR, Christianson TS, Uhrich MA (2015) Estimating concentrations of fine-grained and total suspended sediment from close-range remote sensing imagery. In *SEDHYD 2015*
- Mount R (2005) Acquisition of Through-water Aerial Survey Images. *Photogrammetric Engineering & Remote Sensing* 71(12):1407-1415
- National Water Quality Standards for Malaysia (2019) <https://www.doe.gov.my/portalv1/wp-content/uploads/2019/05/Standard-Kualiti-Air-Kebangsaan.pdf>. Accessed 11 November 2020
- Nebiker S, Annen A, Scherrer M, Oesch D (2008) A light-weight multispectral sensor for micro UAV—Opportunities for very high resolution airborne remote sensing. *The international archives of the photogrammetry, remote sensing and spatial information sciences* 37(B1):1193-1199
- Newcombe CP, Macdonald DD (2011) Effects of Suspended Sediments on Aquatic Ecosystems. *North American Journal of Fisheries Management* 11(1):72-82

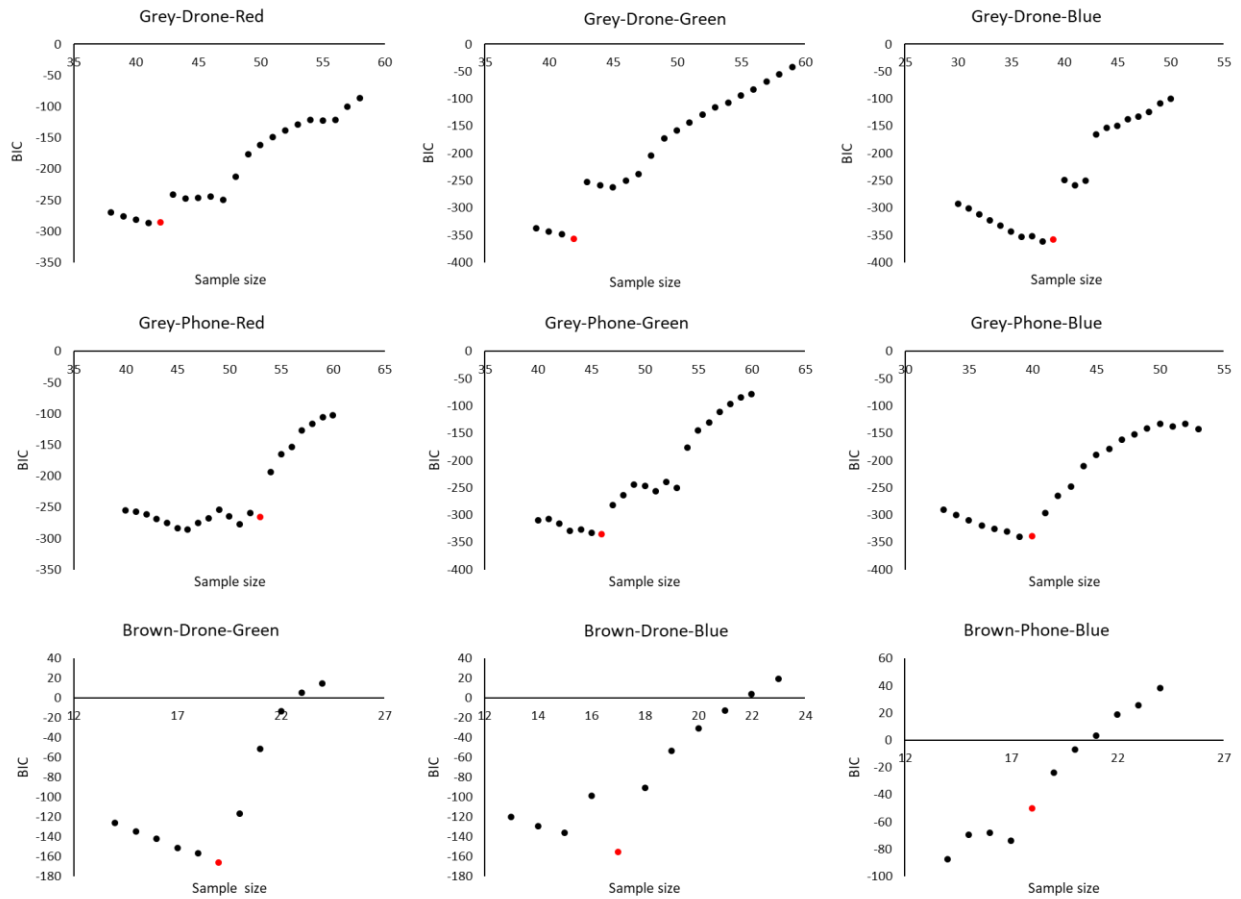
- Nichol JE (1993a) Remote sensing of tropical blackwater rivers: a method for environmental water quality analysis. *Applied Geography* 13(2):153-168
- Nichol JE (1993b). Remote sensing of water quality in the Singapore-Johor-Riau growth triangle. *Remote sensing of Environment* 43(2):139-148
- Nisbet R, Miner G, Yale K (2018) Chapter 7 – Basic Algorithms for Data Mining : A Brief Overview. *Handbook of Statistical Analysis and Data Mining Applications (Second Edition)*, 121-147
- Noe GB, Hupp CR (2009) Retention of riverine sediment and nutrient loads by coastal plain floodplains. *Ecosystems* 12(5):728-746
- Noorazuan MH, Rainis R, Juahir H, Zain SM, Jaafar N (2003) GIS application in evaluating land use-land cover change and its impact on hydrological regime in Langat River basin, Malaysia. In 2nd annual Asian conference of map Asia, 14-15
- Novo EMM, Hansom JD, Curran PJ (1989) The effect of sediment type on the relationship between reflectance and suspended sediment concentration. *Remote Sensing* 10(7):1283-1289
- Nuttall PM (1972) The effects of sand deposition upon the macroinvertebrate fauna of the River Camel, Cornwall. *Freshwater Biology* 2(3):181-186
- Ormerod SJ, Dobson M, Hildrew AG, Townsend C (2010) Multiple stressors in freshwater ecosystems. *Freshwater Biology* 55:1-4
- Othman AK, Othman J, Syed Abdullah SM (2004). Application of remote sensing on the dispersion and concentration of total suspended sediment offshore Langat Estuary. *Sains Malaysiana* 33
- Overstreet BT, Legleiter CJ (2017) Removing sun glint from optical remote sensing images of shallow rivers. *Earth Surface Processes and Landforms* 42(2):318-333
- Owens PN, Batalla RJ, Collins AJ et al (2005) Fine-grained sediment in river systems: environmental significance and management issues. *River research and applications* 21(7):693-717
- Paola C (2000) Quantitative models of sedimentary basin filling. *Sedimentology* 47 :121-178
- Pavanelli D, Palgilarani A (2002) Monitoring water flow, turbidity and suspended Sediment load, from an Apennine catchment basin. *Biosystems Engineering* 83:4
- Pereira FJS, Costa CAG, Foerster S, Brosinsky A, de Araújo JC (2019) Estimation of suspended sediment concentration in an intermittent river using multi-temporal high-resolution satellite imagery. *International Journal of Applied Earth Observation and Geoinformation* 79:153-161
- Pham QV, Ha NTT, Pahlevan N et al (2018). Using Landsat-8 images for quantifying suspended sediment concentration in Red River (Northern Vietnam). *Remote Sensing* 10(11):1841

- Qian Y, Zhang W, Yu L, Feng H (2015) Metal pollution in coastal sediments. *Current Pollution Reports* 1(4):203-219
- R Core Team (2020) R: A language and environment for statistical computing. R Foundation for Statistical Computing, Vienna, Austria. URL <https://www.R-project.org/>.
- Rahman A (2014) Water shortage in Malaysia: Again?. *Malays Consum Law J* 1:115-128
- Reid AJ, Carlson AK, Creed IF et al (2019) Emerging threats and persistent conservation challenges for freshwater biodiversity. *Biological Reviews* 94(3):849-873
- Richardson LL (1996) Remote sensing of algal bloom dynamics. *BioScience* 46(7):492-501
- Ritchie JC, Schiebe FR, McHenry JR (1976) Remote sensing of suspended sediments in surface waters. *Photogrammetric Engineering and Remote Sensing* 42(12):1539-1545
- Ritchie JC, Zimba PV, Everitt JH (2003) Remote sensing techniques to assess water quality. *Photogrammetric engineering & remote sensing* 69(6):695-704
- Robert JH (2020) raster: Geographic Data Analysis and Modeling. R package version 3.3-13. <https://CRAN.R-project.org/package=raster>
- Rochelle-Newall EJ, Fisher TR (2002) Chromophoric dissolved organic matter and dissolved organic carbon in Chesapeake Bay. *Marine Chemistry* 77(1):23-41
- Roslan ZA, Naimah Y, Roseli ZA (2012) River bank erosion risk potential with regards to soil erodibility. *River Basin Management VII* 172:289-297
- Sano EE, Ferreira LG, Asner GP, Steinke ET (2007) Spatial and temporal probabilities of obtaining cloud-free Landsat images over the Brazilian tropical savanna. *International Journal of Remote Sensing* 28(12):2739-2752
- Santos MJ, Khanna S, Hestir EL, Andrew ME, Rajapakse SS, Greenberg JA, ... Ustin SL (2009) Use of hyperspectral remote sensing to evaluate efficacy of aquatic plant management. *Invasive Plant Science and Management* 2(3):216-229
- Schaepman-Strub G, Painter T, Huber S et al (2004) About the importance of the definition of reflectance quantities-results of case studies. In *Proceedings of the XXth ISPRS Congress* :361-366
- Shah SA (October 6 2020) Semenyih River pollution preventable as contaminants visible for years. *The Malaysian Reserve*. <https://themalaysianreserve.com/2020/10/06/semenyih-river-pollution-preventable-as-contaminants-visible-for-years/>. Accessed 11 November 2020
- Shahtahmassebi A, Yang N, Wang K, Moore N, Shen Z (2013) Review of shadow detection and de-shadowing methods in remote sensing. *Chinese Geographical Science* 23(4):403-420
- Shahtahmassebi A, Wang K, Shen Z et al (2011) Evaluation on the two filling functions for the recovery of forest information in mountainous shadows on Landsat ETM+ Image. *Journal of Mountain Science* 8(3):414-426

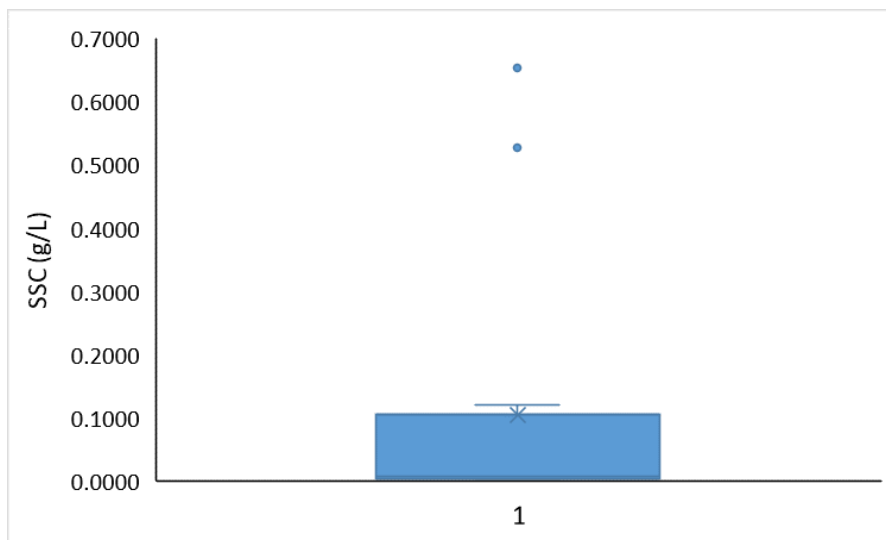
- Shi L, Mao Z, Wang Z (2018) Retrieval of total suspended matter concentrations from high resolution WorldView-2 imagery: a case study of inland rivers. In IOP conference series: Earth and Environmental Science 121
- Suhaila J, Deni SM, Zin WW, Jemain AA (2010) Trends in peninsular Malaysia rainfall data during the southwest monsoon and northeast monsoon seasons: 1975–2004. *Sains Malaysiana* 39(4):533-542
- Sun L, Fang H, Cai Q et al (2019) Sediment load change with erosion processes under simulated rainfall events. *Journal of Geographical Sciences* 29(6):1001-1020
- Swain KC, Thomson SJ, Jayasuriya HP (2010) Adoption of an unmanned helicopter for low-altitude remote sensing to estimate yield and total biomass of a rice crop. *Transactions of the ASABE* 53(1):21-27
- Syvitski JP, Vörösmarty CJ, Kettner AJ, Green P (2005) Impact of humans on the flux of terrestrial sediment to the global coastal. *Ocean Science* 308(5720):376-380
- Syvitski JP, Kettner A (2011) Sediment flux and the Anthropocene. *Philosophical Transactions of the Royal Society A: Mathematical, Physical and Engineering Sciences* 369(1938):957-975
- Talib SHA, Yusoff MS, Hasan ZA (2012) Modeling of sedimentation pattern in Bukit Merah Reservoir, Perak, Malaysia. *Procedia Engineering* 50:201-210
- Teh SH (2011) Soil erosion modeling using RUSLE and GIS on Cameron highlands, Malaysia for hydropower development (Doctoral dissertation).
- Tena A, Batalla RJ (2013) The sediment budget of a large river regulated by dams (The lower River Ebro, NE Spain). *Journal of Soils and Sediments* 13(5):966-980
- Tolk BL, Han L, Rundquist DC (2000) The impact of bottom brightness on spectral reflectance of suspended sediments. *International Journal of Remote Sensing* 21(11):2259-2268
- Tomsett C, Leyland J (2019) Remote sensing of river corridors: A review of current trends and future directions. *River Research and Applications* 35(7):779-803
- Toriman ME, Karim OA, Mokhtar M, Gazim MB, Abdullah MP (2010) Use of InfoWork RS in modeling the impact of urbanisation on sediment yield in Cameron Highlands Malaysia. *Nat Sci* 201(8)
- Triggs R (2020) Why camera sensor size is more important than more megapixels. <https://www.androidauthority.com/camera-sensor-size-1095299/>. Accessed 11 November 2020
- United States Environmental Protection Agency (1999) Method 160.2: Total suspended solids (TSS) (gravimetric, dried at 103–105°C), revised edn. Washington, D.C
- Van Nieuwenhuysse EE, LaPerriere JD (1986) Effects of placer gold mining on primary production in subarctic streams of Alaska. *Journal of the American Water Resources Association* 22(1):91-99

- Vercruyse K, Grabowski RC (2019) Temporal variation in suspended sediment transport: linking sediment sources and hydro-meteorological drivers. *Earth Surface Processes and Landforms* 44(13):2587-2599
- Vogt MC, Vogt ME (2016) Near-remote sensing of water turbidity using small unmanned aircraft systems. *Environmental Practice* 18(1):18-31
- Vörösmarty CJ, Meybeck M, Fekete B et al (2003) Anthropogenic sediment retention: major global impact from registered river impoundments. *Global and Planetary Change* 39(1-2):169-190
- Walling DE (2006) Human impact on land–ocean sediment transfer by the world's rivers. *Geomorphology* 79(3-4):192-216
- Wenger AS, Harvey E, Wilson S et al (2017) A critical analysis of the direct effects of dredging on fish. *Fish and Fisheries* 18(5):967-985
- Wenger AS, Johansen JL, Jones GP (2012) Increasing suspended sediment reduces foraging, growth and condition of a planktivorous damselfish. *Experimental Marine Biology and Ecology* 428:43-48
- Widney S, Klein AK, Ehman, J et al (2018) The value of wetlands for water quality improvement: an example from the St. Johns River watershed, Florida. *Wetlands Ecology and Management* 26(3):265-276
- Witte WG, Whitlock CH, Usry JW, Morris WD, Gurganus EA (1981) Laboratory measurements of physical, chemical, and optical characteristics of Lake Chicot sediment waters. NASA technical paper
- Wood PJ, Armitage PD (1997) Biological effects of fine sediment in the lotic environment. *Environmental Management* 21(2):203-217
- Yadav B, Dai C, Durand MT, Howat IM, Frasson RP (2019) Measurement of River Widths and Heights from ArcticDEM and High-Resolution Satellite Imagery. In AGU Fall Meeting Abstracts 2019:H21N-1950
- Yuan L, Sun J (2011) High quality image reconstruction from RAW and JPEG image pair. In 2011 International Conference on Computer Vision 2158-2165
- Zhang C, Yu ZG, Zeng GM et al (2014) Effects of sediment geochemical properties on heavy metal bioavailability. *Environment International* 73:270-281
- Zhu W, Yu Q, Tian, YQ, Becker BL, Zheng T, Carrick HJ (2014) An assessment of remote sensing algorithms for colored dissolved organic matter in complex freshwater environments. *Remote Sensing of Environment* 140:766-778

Appendices



Appendix 1. BIC-Sample size plots. Red dots indicate the point at which the threshold occurs indicated by a large jump in BIC value.



Appendix 2. Box plot of the 14 SSC values collected in the field.